Freeing Ammonia: Anaerobic degradability of proteins in the presence of multiple carbon sources

Fabian Bodenlenz

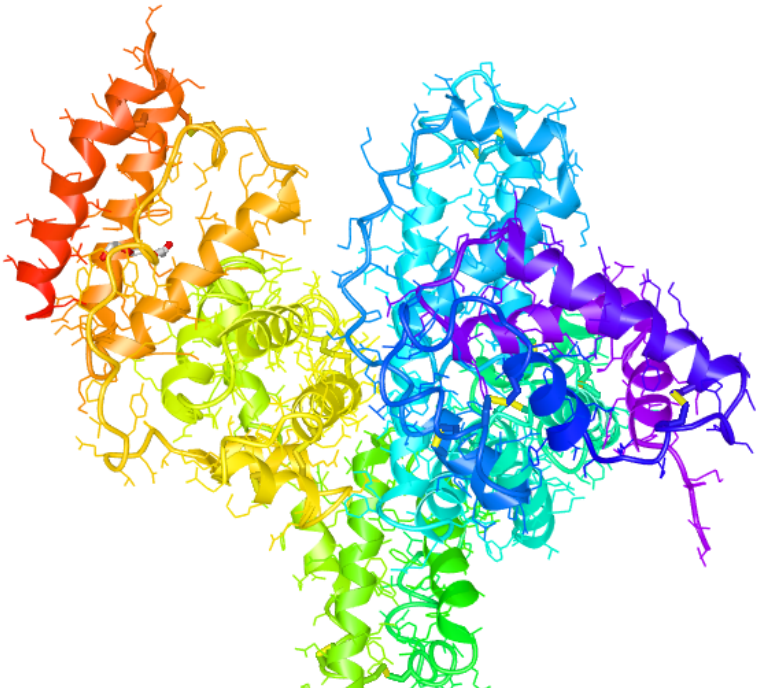

TU Delft

FREEING AMMONIA: ANAEROBIC DEGRADABILITY OF PROTEINS IN THE PRESENCE OF MULTIPLE CARBON SOURCES

A thesis submitted to the Delft University of Technology in partial fulfillment of the requirements for the degree of

Master of Science in Civil Engineering

by

Fabian Bodenlenz

to be publicly defended on February 21, 2020 at 13:00

The work in this thesis was made in collaboration with:

Department of Sanitary Engineering
Faculty of Civil Engineering and Geosciences
Delft University of Technology

Student number:	4716833
Daily supervisor:	Ir. Zhe Deng
Thesis committee:	Dr. Ir. Henri Spanjers, chair
	Prof. Dr. Ir. Jules Van Lier
	Dr. Ir. David Weissbrodt

An electronic version of this thesis is available at http://repository.tudelft.nl/.

ABSTRACT

Large nitrogen emissions and depositions in countries like The Netherlands have had a negative impact on human health and natural ecosystems. Nitrogen ends up in water bodies where it causes eutrophication, which can lead to a decrease in biodiversity. Nowadays, it is removed from water at wastewater treatment plants (WWTPs) via denitrification – nitrification or the anammox process. In both of these processes the end product is N_2 gas, which is again emitted into the atmosphere.

In recent years, however, nitrogen in the form of ammonia (NH_3) has received increased attention as a valuable resource and can be found in different types of wastewaters. To produce energy from ammonia, solid oxide fuel cells (SOFCs) are used, to which ammonia should be fed in its gaseous form. For the production of ammonia from wastewater, a low carbon-to-nitrogen ratio is desired. The overall goal of the research project is to identify nitrogen-rich wastewaters from the industry and apply a series of treatment steps for the production of ammonia. Protein-rich wastewaters are especially suitable for the production of ammonia. Effluents fitting these criteria have been identified, so far, in several industrial settings, namely the slaughterhouse, food and dairy industry.

Proteins can be converted to ammonia through anaerobic digestion, while producing biogas in the form of carbon dioxide (CO_2) and methane (CH_4), which can also be used for energy purposes. Next to proteins, carbohydrates and volatile fatty acids (VFAs) also make part of protein-rich wastewater. However, not a lot is known about the co-digestion of proteins and these simple carbon sources. Some aspects have been investigated, but thorough research on the whole degradation is needed to fully understand the process.

The master thesis research presented in this report focused on the anaerobic degradability of proteins in the presence of sugars and VFAs. Three proteins (bovine serum albumin [BSA], casein and gelatin) were selected from the identified industries and assessed based on degradation efficiency and kinetic rates, under mesophilic batch test conditions. Furthermore, the conversion of protein to ammonia was assessed and parameters to define a biological ammonia potential (BAP) are defined.

An increase in the degradation coefficient after the co-digestion with sugar was observed for gelatin (1.1 to 1.6 d^{-1}) and BSA (0.57 to 0.68 d^{-1}). Pure proteins were degraded efficiently with 71 - 96% compared to 76 - 97% of the co-digested batches. A combination of conversion efficiencies and the newly introduced biological ammonia potential gave a good indication on the conversion of protein to NH_4^+. Acidification with VFAs resulted in process instabilities with respect to the methane production rate, which was due to the applied ratio of propionate to acetate. To prevent this in future trials, amino acid analysis to predict the production of VFAs from protein was evaluated with a maximum deviation of 14% of measured to theoretical values.

This study demonstrated the efficiency of co-digestion to degrade protein-rich substrates. Further research is required to unveil the impact of high ammonia concentrations and explore the microbiological aspect of protein fermentation. Finally, considerations for a test to assess the biological ammonia potential are given.

ACKNOWLEDGEMENTS

I would not have been able to finish this research project without the help of a great amount of people.

First and foremost, I want to thank Ir. Zhe Deng, my daily supervisor, for your great help throughout the project. Your way of guiding me through my research helped me to reflect more critically on my results as well as putting together the individual pieces of the puzzle. I wish you all the best for your further PhD endeavors. I would also like to thank Dr. Ir. Henri Spanjers. Your curiosity helped me to discover more areas of interest within my project and I am very grateful for your input and being able to work with you on several occasions.

I would also like to express my gratitude to my other committee members. Prof. Dr. Ir. Jules van Lier, you always had an open ear to discuss theories and set up hypotheses. No matter which aspect of the project we were discussing, you were aware of the details, which improved my work a lot. To Dr. Ir. David Weissbrodt, I want to thank you for the great commitment you put into all of our meetings. I believe every meeting we had exceeded the planned 45 minutes by at least 30 minutes; you always go an extra mile for your students, which I profited from greatly.

During my thesis, I had the opportunity to work at the facilities at Biothane in Delft. I would like to thank Dr. Ana Lucia Morgado Ferreira and Dr. Santiago Pacheco-Ruiz for their guidance throughout my time at Biothane. You triggered me to think more of the applicability of my findings, which brought a lot of additional value to my development in a research environment. I also want to thank the laboratory team, Patrick van der Linde and Menno Lam, who helped me tremendously with the set-up and measuring devices.

Furthermore, I would like to thank Patricia van den Bos, who put a lot of effort into developing a new method for measuring amino acids at the Waterlab at TU Delft. We spent a lot of time with the HPLC-MS and I am glad we managed to make it work.

I would also like to thank my parents and siblings for their love and support during all my studies. Even if the distance is far, you never hesitated to accept my choices and help me in every way you can.

Lastly, I want to thank my friends. I felt at home here in Delft with you and I cherish all the moments that we shared. A special thanks goes to Akshay, Ashwini, and Sanne for reading my report. Furthermore, I would like to thank Alessandro, Chris, and Julia for their support, especially towards the end of my project.

CONTENTS

LIST OF FIGURES

LIST OF TABLES

ABBREVIATIONS

List of Abbreviations

AD	Anaerobic Digestion
ATP	Adenosine triphosphate
BA	Biological Acidification
BAP	Biologial Ammonia Potential
BCA	Bicinchoninic Acid
BD	Biodegradability
BMP	Biomethane Potential
BSA	Bovine Serum Albumin
CE	Conversion Efficiency
COD	Chemical Oxygen Demand
COD_{VFAs}	Chemical Oxygen Demand of volatile fatty acids
Da	Dalton [unified atomic mass unit]
GC	Gas Chromatography
HRT	Hydraulic Retention Time
SCOD	Soluble Chemical Oxygen Demand
SKN	Soluble Kjeldahl Nitrogen
SOFC	Solid Oxide Fuel Cell
TAN	Total Ammoniacal Nitrogen
tCOD	Total Chemical Oxygen Demand
TKN	Total Kjeldahl Nitrogen
VFA	Volatile Fatty Acid
VS	Volatile Solids
AA	Amino Acid
Ala (A)	Alanine
Arg (R)	Arginine
Asn (N)	Asparagine
Asp (D)	Aspartic Acid
Cys (C)	Cysteine
Gln (Q)	Glutamine
Glu (E)	Glutamic Acid
Gly (G)	Glycine
His (H)	Histidine
Ile (I)	Isoleucine
Leu (L)	Leucine
Lys (K)	Lysine
Met (M)	Methionine
Phe (F)	Phenylalanine
Pro (P)	Proline
Ser (S)	Serine
Thr (T)	Threonine
Trp (W)	Tryptophan
Tyr (Y)	Tyrosine
Val (V)	Valine

1 INTRODUCTION

This chapter attempts to illustrate the relevance of the conducted research project and ends with a rough outline of the research plan.

1.1 STIKSTOFPROBLEMATIEK OR: THE HUMAN IMPACT ON THE NITROGEN CYCLE

Humankind has - in a relatively short time span - doubled the supply of reactive nitrogen on Earth, and it is projected to continue growing in the near future (Galloway [1998]). This anthropogenic fixation of nitrogen has caused an imbalance in the nitrogen cycle, which triggers health and environmental problems alike (Townsend et al. [2003]). Especially in the Netherlands, the "Stikstofproblematiek" (nitrogen problem) has been discussed thoroughly due to the fact that its nitrogen deposition rates were once the highest in the world with an average of 2900-6400 $molN \cdot ha \cdot yr^{-1}$ in 1997, which decreased to 1730 $molN \cdot ha \cdot yr^{-1}$ in 2018 (Vitousek et al. [1997]; Hoogerbrugge et al. [2019]). Figure 1.1 shows the processes included in global nitrogen fixation. Specifically for the Netherlands Figure 1.2 shows the sources of nitrogen depositions from 2018.

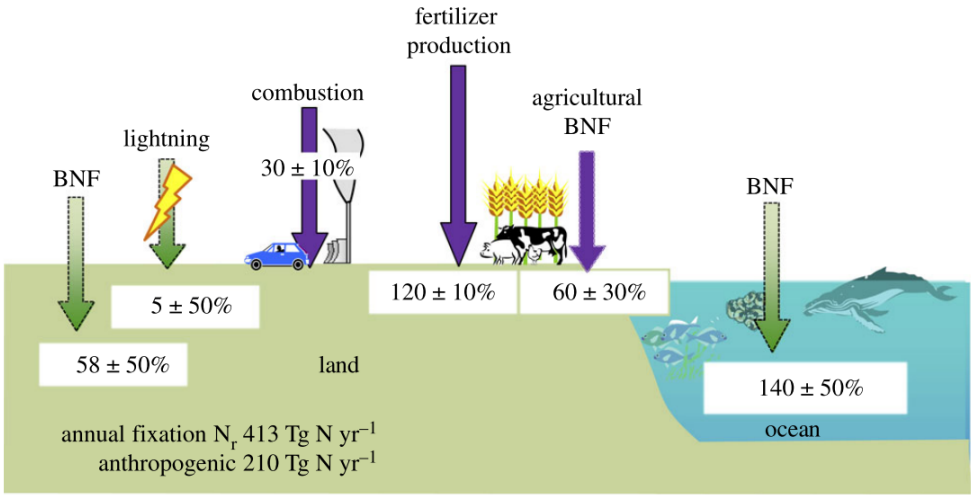

Figure 1.1: Different processes combine to the global nitrogen fixation, such as lightning, combustion, fertilizer and industrial production via the Haber-Bosch process as well as biological nitrogen fixation (BNF). The displayed data is for the year 2010. Arrows show a transfer from atmospheric N_2 to ecosystems of terrestrial or marine origin. Green depicts natural whereas purple arrows stand for anthropogenic sources, which make up more than 50% of all sources. Retrieved from Fowler et al. [2013].

As already mentioned, one of the main issues of nitrogen fixation is of environmental nature. This includes, for example, the eutrophication of water bodies, which can lead to a decrease in biodiversity (Townsend et al. [2003]). To prevent this, nitrogen is removed in municipal and industrial wastewater treatment plants either via nitrification and denitrification or the less energy-intense anammox pro-

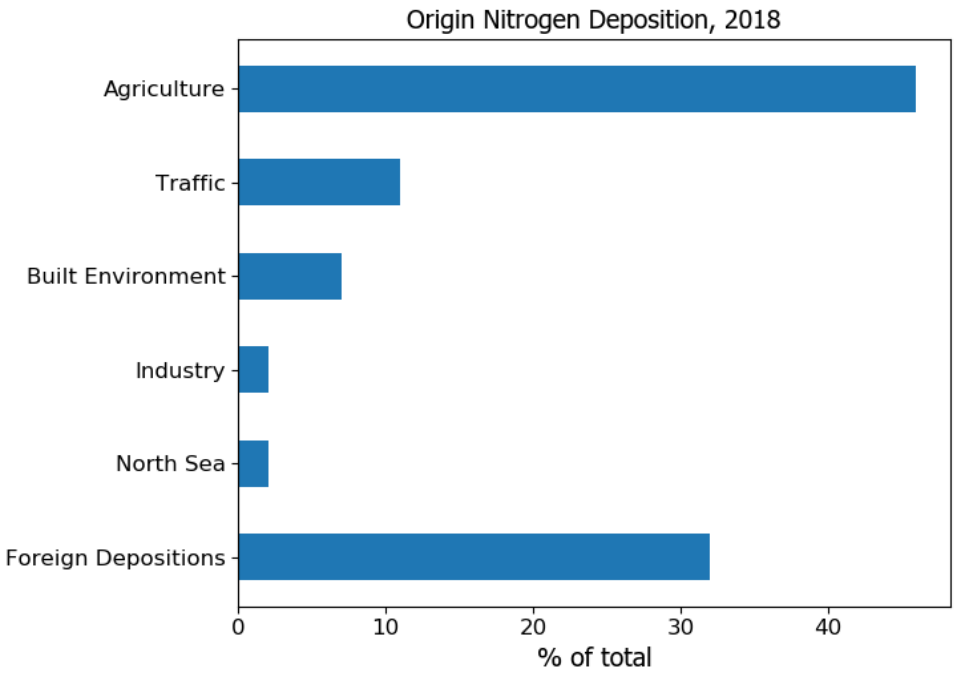

Figure 1.2: Nitrogen depositions in the Netherlands mainly arise from agriculture (46%), followed by depositions originating from outside the country (32%). Traffic (11%) includes road traffic, international ship traffic and other traffic. The built environment (7%) entails households, construction, authorities, trade and services. The industry (2%) combines industrial processes, the energy sector, waste processing and refineries. Data retrieved from Hoogerbrugge et al. [2019]; Klein et al. [2019].

cess (Chang et al. [2018]). However, even though the anammox process seems as a viable alternative, the end product for both treatment processes is N_2 gas, which is subsequently released into the atmosphere. Thus, the problem of N_2 emission is not solved and an alternative is desired.

1.2 NITROGEN AS A RESOURCE

Recently, more and more research is aimed at evaluating ammonia (NH_3) as a resource (Wang [2018]; Chang et al. [2018]; Valera-Medina et al. [2018]). By converting nitrogen compounds in wastewater to ammonia it can be used in power cycles, fuel cells or combustion based technologies (Valera-Medina et al. [2018]). The main reasons for its consideration are the reduction of costs, emissions and the securing of an abundant resource (Chang et al. [2018]; Valera-Medina et al. [2018]).

For the application in wastewater treatment, fuel cells can be used for the generation of energy. These can be either conventional such as solid oxide fuel cells (SOFCs) or even biological such as microbial fuel cells (MFCs) (Chang et al. [2018]; Valera-Medina et al. [2018]). However, due to a mix of substances in the wastewater, such as heavy metals, organics or toxic pollutants, the conversion of nitrogenous compounds to ammonia and subsequent recovery thereof can be difficult to achieve (Chang et al. [2018]).

For SOFCs, wastewaters with a low carbon-to-nitrogen (C:N) ratio in the range of 3-10 are preferred to maximise the generation of ammonia, which, however, also increases the production of VFAs due to retarded degradation resulting from free ammonia toxicity (Lin and Xu [2019]). In industrial systems, water with a low C:N ratio comes from a variety of different disciplines, such as the slaughterhouse, dairy,

or tannery industry. However, to make the nitrogen available for a fuel cell a series of pre-treatments is needed.

A collaboration between Delft University of Technology and Biothane Delft investigates strategies to produce energy from ammonia of nitrogen-rich wastewater. In a first step, wastewaters with a low C:N ratio as well as high organic content are identified. Then, anaerobic digestion is chosen as a means of degrading organic material in wastewater due to low energy input and simultaneous production of biogas. Consequently, total ammoniacal nitrogen (TAN) is present in its ionised or unionised form (NH_4^+ or NH_3), which needs to be concentrated and made accessible for the fuel cell. The overall structure of this research project is displayed in Figure 1.3. The part that is addressed in this research project is highlighted in red.

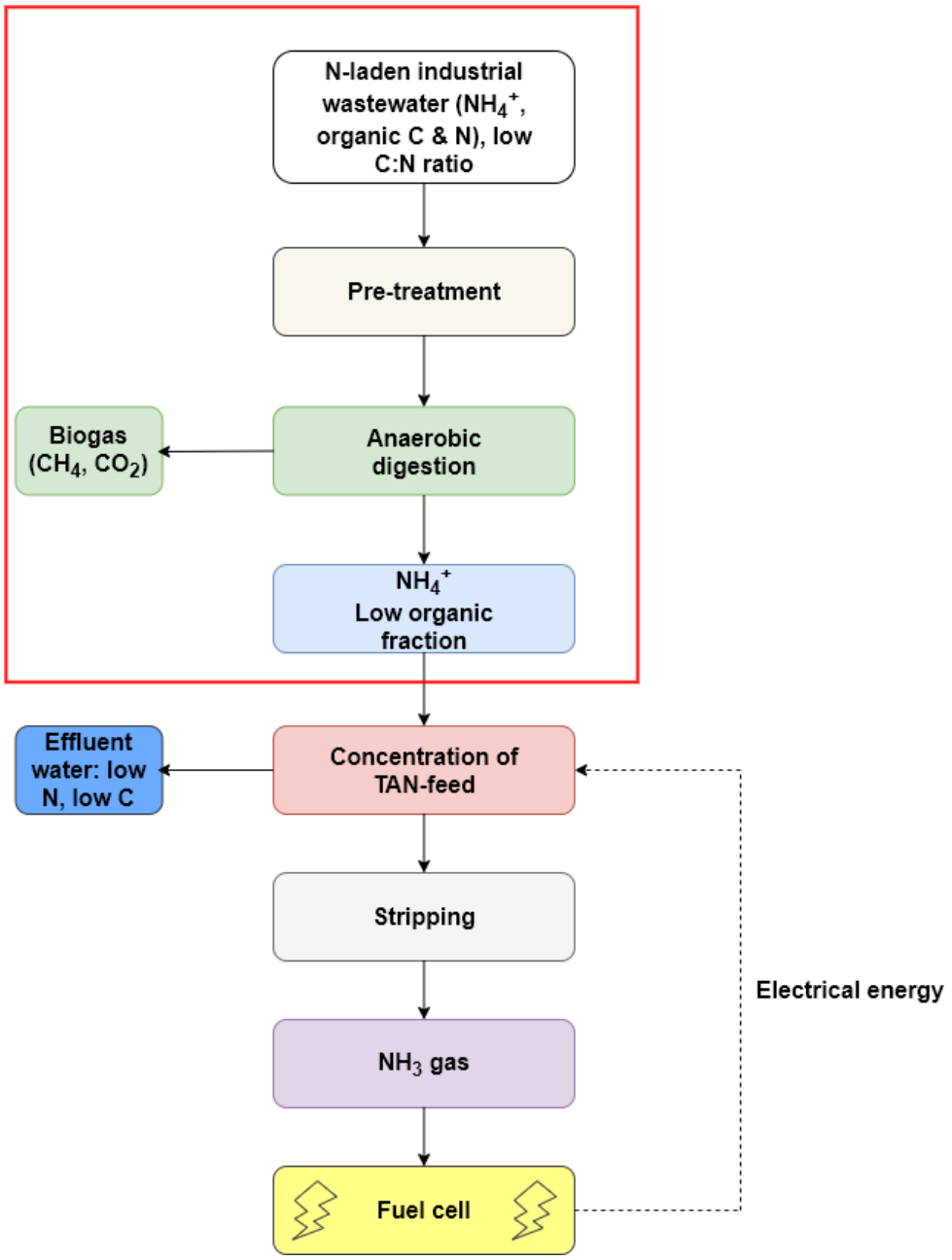

Figure 1.3: Conceptual scheme of the treatment steps for the extraction and recovery of NH_3 within the bigger research project. The steps which this thesis is focussing on are outlined in red.

1.3 RESEARCH PLAN

This thesis investigates co-digesting proteins and additional carbon sources, in the form of sugar and volatile fatty acids, to improve the degradability of proteins. The aim is to determine if both the methane yield and production rate as well as protein degradation rate and efficiency can be improved through co-digestion. Three proteins, gelatin, BSA and casein were investigated in the combination with glucose for gelatin and BSA, and lactose for casein. These combinations were compared to pure protein digestion.

In a subsequent step, biological acidification is applied on the present carbohydrates. This means that part of the (sugar) feed is added as volatile fatty acids (VFAs) in order to mimic the process in a two-phase reactor. Therefore, the supplied carbon sources will be propionate and acetate (the main VFAs) and again the digestion process is analysed based on methane production as well as protein degradation.

To interpret the NH_4^+ production from proteins, an attempt was made to define parameters directly related to protein conversion. This was done in order to define how biologically produced ammonia can be assessed.

2 LITERATURE REVIEW

This chapter gives the theoretical background collected through a thorough literature study. In each section a topic will be touched upon, which combined, gives the required knowledge to develop the approach for this research project. Next to established knowledge, the identified gaps will be highlighted.

2.1 PROTEINS: STRUCTURE AND DEGRADATION

Proteins are macromolecules that can be found in most living organisms. They are carriers of different compounds that vary in size from bigger molecules to electrons. Proteins play important roles in organisms such as guiding flows of electrons or balancing hormonal release, which make them indispensable in a multitude of processes (Creighton [1993]).

In the following sections an overview is given to understand

- the chemical and structural properties of proteins and their building blocks
- important mechanisms of protein degradation
- the relation between proteins and wastewater
- the combined degradation of proteins and carbohydrates

Then, the three proteins investigated in this research are discussed in more detail in terms of occurrence, structure and peculiarities.

2.1.1 Chemical and structural properties of amino acids and proteins

Proteins show more complexity than other polymers, such as polysaccharides, due to the fact that they can incorporate 20 different monomers, also called amino acids, in their structure (Creighton [1993]; Berg et al. [2006]). By varying the arrangement and length of the amino acid sequence a distinction between individual proteins can be made. Nearly all amino acids have a general structure in common, with a central carbon atom also called α-carbon, linked to an amino (NH_2) group, a carboxyl ($COOH$) group, a hydrogen atom and a distinctive R group (Berg et al. [2006]). These building blocks can form longer chains through a condensation reaction to form a **peptide**. The order in which they are arranged is written in the genes of the specific organism that produces the protein.

An amino acid in the resulting peptide is termed a **residue**, and several peptides linked to each other are known as **polypeptide**. As soon as polypeptides interact through noncovalent bonds, the folding sets in and the resulting structure is known as **protein** (Creighton [1993]; Berg et al. [2006]; Walsh [2014]; Brigham [2018]). The general structure of a peptide bond as well as its formation are depicted in Figure 2.1.

At a pH between $5 - 9$, amino acids are present in dipolar form, which is called zwitterionic state. This means that both the amino group (NH_3^+) and the carboxyl group (COO^-) are present in their charged form, resulting in a net charge of zero. This state changes as the pH de- or increases (Berg et al. [2006]).

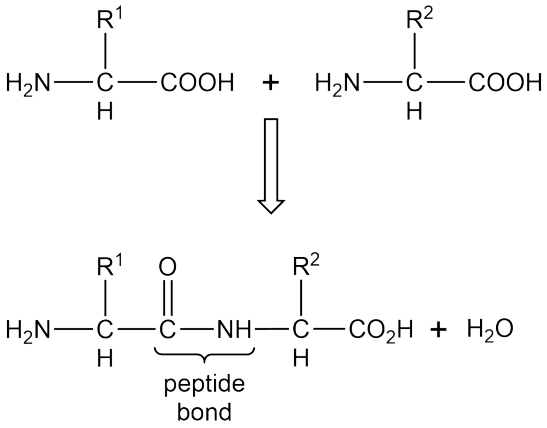

Figure 2.1: The condensation reaction between two amino acids creates a peptide bond that links the amino group of one with the carboxyl group of the other acid.

The R group, or side chain, is what is distinctive for each amino acid. This side chain can be as simple as a single hydrogen atom as in the case of glycine, or as complex as in the case of tryptophan, which comprises of two fused aromatic rings containing an NH group (Berg et al. [2006]). In Figure 2.2 a list of all 20 natural amino acids including their structure is shown.

The structure of a protein can be described on several levels, namely primary, secondary, tertiary and quaternary. The arrangement of amino acids within a polypeptide is known as the primary structure.

Next, the secondary structure relates to the spatial conformation of a polypeptide, excluding side chains of amino acids. There are specific structures that are observed in proteins, such as the α-helix, β sheets or the β turn and Ω loop. The reason for the occurrence of this type of structure is the maximisation of stability through intramolecular hydrogen bonds and the simultaneous reduction of steric repulsion between adjacent side-chain groups (Berg et al. [2006]; Walsh [2014]).

The tertiary structure of proteins refers to the three-dimensional orientation of a protein or polypeptide, and the interaction of amino acid residues that are further apart in the sequence. In that way, a protein can be folded to, for example, reveal polar residues whereas nonpolar residues are buried within the interior to increase the polarity of the protein itself. If several polypeptide chains fold into different directions they form so-called **domains** that can incorporate between 30 and 400 amino acid residues (Berg et al. [2006]).

Finally, the quaternary structure refers to the spatial arrangement of several polypeptide chains in one protein, which are called **subunits** (Creighton [1993]; Berg et al. [2006]; Walsh [2014]). However, the proteins investigated in this research do not show any quaternary structure.

2.1.2 Degradation pattern of proteins and amino acids

The process of breaking down a protein into smaller polypeptides, peptides and amino acids is called **proteolysis**. It is induced by cellular enzymes called proteases, which hydrolyse the peptide bonds shown in Figure 2.1. This is followed by restoring the carboxyl component of one and the amino component of the other amino acid (Berg et al. [2006]). An important parameter determining the breakdown rate is the type of amino-terminal residues. A study conducted in 1991 states that a categorisation can be attempted based on the half-lives of N-terminal residues. The distinction was made between highly stabilising residues with a half-life of more than 20 hours and destabilising residues with a half-life of less than 30 minutes (Tobias et al. [1991]; Varshavsky [1996]).

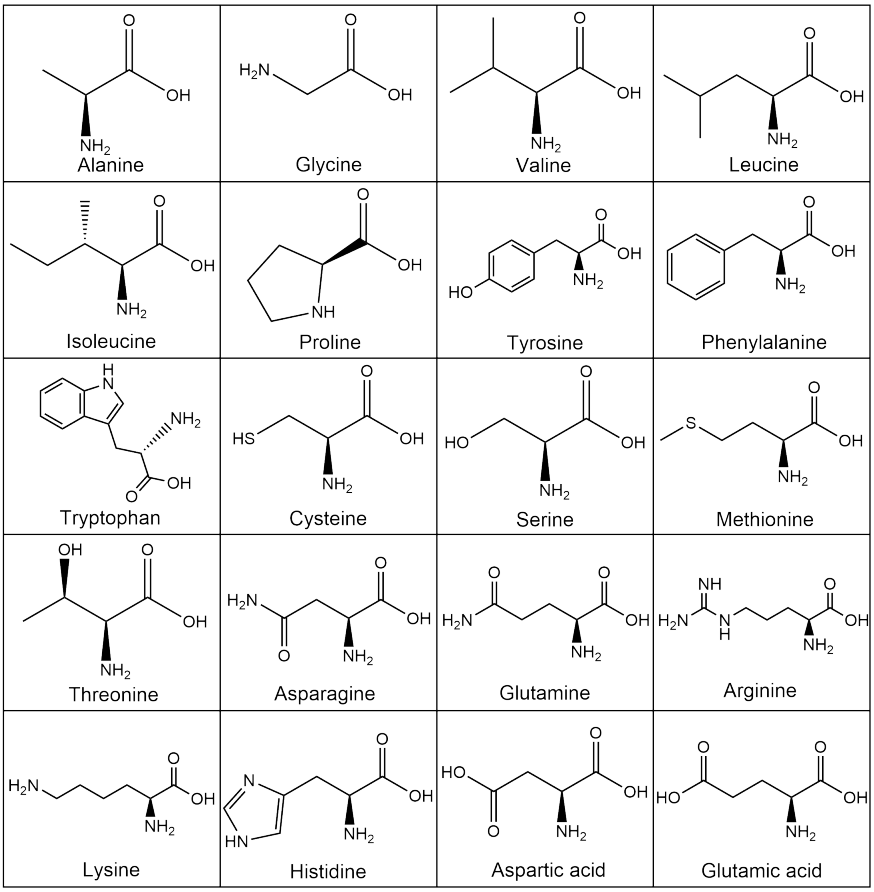

Figure 2.2: Skeletal formulas of all 20 amino acids found in proteins. A further categorisation can be made according to the side-chain structure (Berg et al. [2006]).

After the cleavage of peptide bonds, amino acids are released and can further ferment via two distinct reactions: coupled redox reactions, also called Stickland reactions, or single amino acid fermentation, which requires the presence of hydrogen-utilising bacteria. During the Stickland reaction, one amino acid acts as an electron donor (the product is shorter by one carbon atom than the original amino acid), and the other as electron acceptor (the product does not change in number of carbon atoms to the original). During this process NH_3 is released (Ramsay and Pullammanappallil [2001]). It is reported that fermentation via the Stickland reaction occurs faster than single amino acid fermentation. In total there are five amino acids, which can act as both electron donor and acceptor. Per mole of amino acid fermented via the Stickland reaction, the cell gains 0.5 mole of ATP (Barker [1981]).

In contrast, the less common single amino acid fermentation occurs with hydrogen as either reactant or product. This reaction can be slowed down if a saturation of hydrogen is reached (Nanninga and Gottschal [1985]).

2.2 PROTEINS IN INDUSTRIAL WASTEWATER

Industrial wastewaters from various industries show high concentrations of proteins. Substantial amounts of protein can be found in effluents of the slaughterhouse, dairy and the tanning industry. When speaking of high concentrations, usually high-strength wastewaters display a tCOD of up to 10 000 mg/L. With proteins making up around 30% of the tCOD the protein content of these types of wastewa-

ter is around 3000 $mgCOD \cdot L^{-1}$ (Lin et al. [2017]). An overview of the occurrence of different proteins is given in Table 2.1.

An important parameter of proteins in wastewater is their isoelectric point, which is reached at the pH at which the net charge is zero. At this pH, a protein's electrophoretic mobility is zero, which means that intermolecular interactions decrease and Van der Waals forces increase to the point where the protein forms small clusters that precipitate (Berg et al. [2006]; Bhat et al. [2016]). This point is inherent for each protein.

Table 2.1: The most relevant proteins and their occurrence together with their main industries are depicted.

Name	Occurrence	Industry
Casein	Milk, cheese	Dairy
Collagen	Skin	Tanning, leather
Gelatin	Irreversibly hydrolysed version of collagen	Meat processing
Serum albumin	Blood protein	Slaughterhouse
Albumen	Egg white compound	Food processing

The following subsections will highlight the proteins casein, gelatin, and serum albumin that are displayed in Table 2.1. First, their structural properties will be addressed, followed by an illustration of the ratio of amino acids and individual peculiarities of each protein. In a last step, the degradation pattern of proteins in the presence of carbohydrates will be addressed. Carbohydrates are, in the case of the chosen proteins, the main compounds found in wastewater, which is why this topic is addressed.

2.2.1 Gelatin

Gelatin is a hydrolysed form of collagen, the main structural protein in the connective tissues in the body of mammals. Collagen is mainly extracted from cattle bones, hides and porkskins (GMIA [2019]). It consists of three monomer units of α-chains, also called trimer, of which each has a molecular mass of around 100 000 Da. If collagen is decomposed, for example through heating, the three chains are broken up by enzymes (partially or completely) and hence form gelatin. Therefore, gelatin is referred to as "derived protein", or polypeptide. As a polypeptide, gelatin does not show all of the typical structural properties of proteins that were described in Section 2.1.1. Furthermore, the molecular weight from collagen to gelatin is drastically reduced to around $1400 - 26000$ Da (Brigham [2018]). Gelatin reaches its isoelectric point at a pH of 4.95.

The main amino acids in both collagen and gelatin are glycine, proline, hydroxyproline and glutamate based on mass. Figure 2.3 shows the composition of all amino acids present in gelatin. The ratio of amino acids is listed in Appendix A.1 (Table A.1).

Due to its gel strength and viscosity, gelatin has various applications in the food industry. Next to being a constituent in "gummy" candy products, gelatin can also be used as thickening agent in ice creams, yoghurt, marshmallows, baking products, etc. Additionally, the pharmaceutical industry produces pills and capsules, which are usually coated with gelatin to aid in swallowing (Brigham [2018]). Gelatin loses its gelling properties and viscous structure if it is heated above approximately 40°C (GMIA [2019]), which is advantageous in wastewater treatment.

2.2.2 Bovine Serum Albumin (BSA)

Serum albumins are the most common proteins in blood, making up around 55% of the total composition. Serum albumin in the blood of cattle, more specifically from

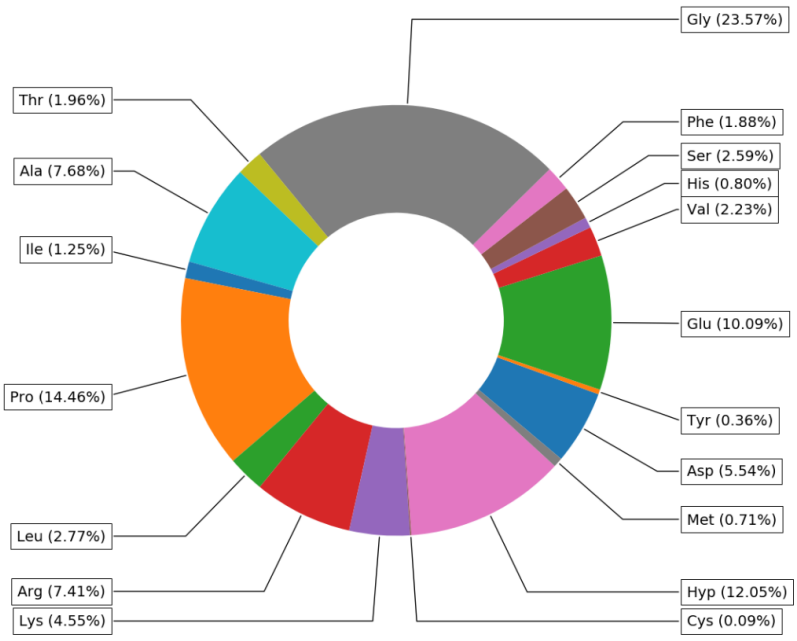

Figure 2.3: Amino acid composition of gelatin from porkskin. The composition is shown in percentages based on dry weight gelatin. The composition of amino acids is taken from the Gelatin Handbook of the Gelatin Manufacturers Institute of America (GMIA [2019]).

domesticated cattle of the species *bos taurus*, is called bovine serum albumin (BSA). The BSA molecule has a heart-shaped form, which consists of three homologous α-helical domains. In total, BSA consists of 607 amino acids of which the first 24 belong to the signal peptide and propeptide, and the following 583 amino acids make up the primary sequence of BSA. The main amino acids of BSA based on mass are glutamate, leucine and lysine, which make up roughly one third of the whole sequence. The composition of all amino acids is shown in Figure 2.4. The whole sequence is listed in Appendix A.1. BSA has a mass of 76800 Da and reaches its isoelectric point at a pH of 4.7. Due to its presence in cattle blood it is also one of the major proteins in slaughterhouse wastewater.

Owing to its inert nature BSA is used in a variety of biochemical assays, such as the bicinchoninic acid kit (BCA) for the determination of proteins in solutions (Mehmood et al. [2019]).

2.2.3 Casein

It is known that dairy wastewater as high-strength wastewater is difficult to degrade (Hassan and Nelson [2012]). This is mainly due to its composition of fat, lactose, and proteins. The ratio of these compounds varies significantly based on the source of dairy wastewater, such as cheese, butter, milk, ice cream, etc. (Baskaran et al. [2003]; Perna et al. [2013]; Traversi et al. [2013]). The two main proteins present in dairy wastewater are casein (75-80%) and whey (or serum) proteins. While whey proteins are rather soluble, casein is of hydrophobic nature and therefore mostly present in particulate form (Hassan and Nelson [2012]). In a biochemical context, casein is referred to as a micelle, which is a complex that includes several types of proteins, namely α_{S1}-, α_{S2}-, β-, and κ-casein (Bhat et al. [2016]). The main difference between these four types of casein is the number of phosphate groups per mole of casein. This also leads to a difference in the isoelectric point, which varies from 4.1 to 5.8.

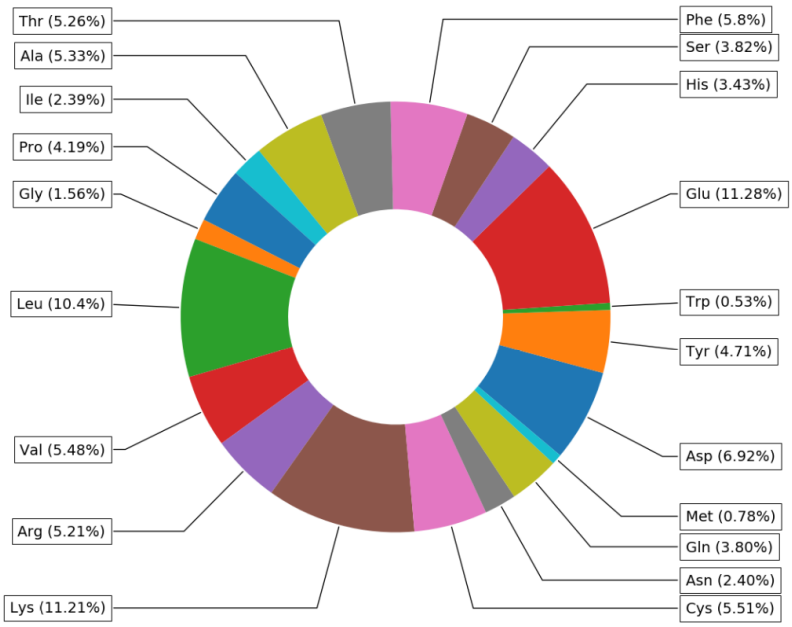

Figure 2.4: Amino acid composition of BSA. The composition is shown in percentages based on the molecular weight of amino acids in the sequence of its primary structure. The composition of amino acids is taken from the UniProt Consortium (2019) (Consortium [2019]).

Structure-wise, the different proteins do not show a well-defined secondary or tertiary structure, and even the primary amino acid sequence of each casein protein differs slightly (Bhat et al. [2016]). Casein consists of a sequence of 225 amino acids, where the first 15 amino acids belong to the signal peptide, and the last 11 form an antioxidant peptide (Consortium [2019]). This leaves 199 amino acids that define the major structure of the protein. Its main amino acids based on mass are glutamate, leucine, lysine and glutamine. Figure 2.5 shows the exact composition of amino acids in casein.

2.2.4 Protein degradation in the presence of carbohydrates

Not a lot is known about the degradation of proteins together with carbohydrates. In earlier studies, a decrease in enzyme production responsible for the hydrolysis of proteins, also called proteases, after the addition of glucose to gelatin feed was assumed (Breure et al. [1986]), which resulted in a decrease of gelatin degradation. Moreover, a decrease in protein degradation was observed after the addition of a mixture of starch and carbohydrates (Tommaso et al. [2003]). In a fairly recent study, however, a positive impact on the degradation rate was observed for a mixture of BSA and starch (Elbeshbishy and Nakhla [2012]).

Considering that those are all different combinations of polypeptides/proteins and carbohydrates/sugars, there is no consensus amongst researchers on the general behaviour of proteins during anaerobic co-digestion. However, it is known from the field of food technology, that an interaction between amino acids and sugars can occur, which is called Maillard reaction, named after its discoverer.

The Maillard reaction occurs between the carbonyl group of sugars and the amino group of amino acids, and can decrease the breakdown of both groups while, simultaneously, nitrogen-containing byproducts, such as melanoidins, are formed. Usually, this reaction occurs at an increased temperature above 100°C, but it also takes place - to a smaller extent - at lower temperatures (Lin et al. [2018]).

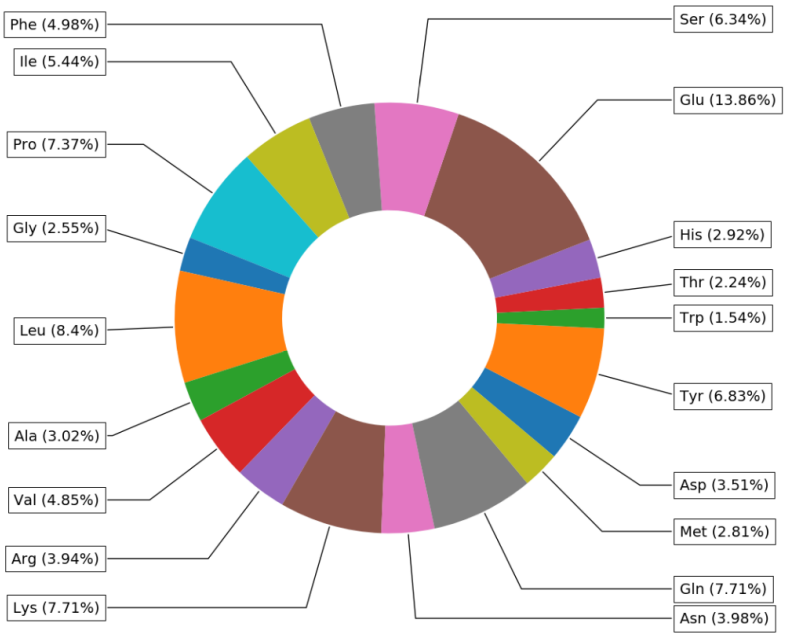

Figure 2.5: Amino acid composition of casein. The composition is shown in percentages based on the molecular weight of amino acids in the sequence of its primary structure. The composition of amino acids is taken from the UniProt Consortium (2019) (Consortium [2019]).

Considering the reported literature in this section, it becomes apparent that clear conclusions on the degradation, both in terms of rate and efficiency, are missing.

To get a more holistic understanding of the protein degradation, the processes of anaerobic digestion are shown in the following section (2.3).

2.3 ANAEROBIC DIGESTION

In general, anaerobic digestion (AD) comprises of four major degradation steps: hydrolysis, acidogenesis, acetogenesis and methanogenesis where each process affects different compounds (van Lier et al. [2008]). Figure 2.6 shows an overview of the processes.

As can be seen in Figure 2.6, particulate matter is grouped into polysaccharides, lipids and proteins. To understand the processes of AD better, a more detailed description of each disintegration step is given here (Pavlostathis and Giraldo-Gomez [1991]; Alexiou [1998]; Kalyuzhnyi et al. [2002]):

1. Hydrolysis: During this first step, hydrolysing bacteria which excrete enzymes are responsible for the breakdown of carbohydrates, proteins and lipids. Polysaccharides degrade to monosaccharides, proteins to amino acids, and lipids into glycerol and long-chain fatty acids. This is considered the rate-limiting step in the AD process and is a surface phenomenon.

2. Acidogenesis: Monosaccharides and amino acids consequently degrade to mixed organic acids (mainly short-chain fatty acids), H_2, CO_2 and NH_3.

3. Acetogenesis: Acetate, H_2 and CO_2 form due to the degradation of long-chain fatty acids, valerate, butyrate and propionate during acetogenesis. One methanogenic group utilises hydrogen produced during the aforementioned step while acetate is utilised by an aceticlastic methanogenic group.

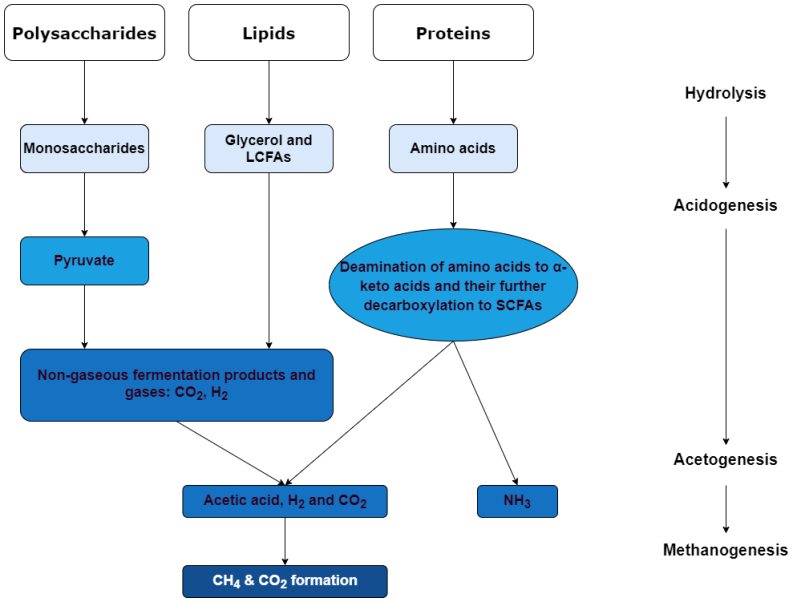

Figure 2.6: Processes involved in anaerobic digestion from macromolecules (top) to the final product biogas (bottom). Products (boxes) are highlighted in the same colour if they are produced during the same process.

4. Methanogenesis: Methanogenic archaea use acetate, H_2 and CO_2 to produce methane during the final step of AD. There are two distinct methanogenic pathways:

   the acetoclastic pathway (equation 2.1)

$$CH_3COOH \rightarrow CH_4 + CO_2 \tag{2.1}$$

   and the hydrogenotrophic pathway (equation 2.2).

$$CO_2 + 4H_2 \rightarrow CH_4 + 2H_2O \tag{2.2}$$

   The methyl group of acetic acid is reduced to methane (CH_4) by acetoclastic methanogens, whereas the carboxylic group is oxidized to CO_2. Considering all methane that is produced during AD, 70% comes from these microorganisms (van Lier et al. [2008]).

Protein-rich wastewater, however, poses a lot of problems as far as anaerobic digestion is concerned. One of the major issues is its degradation product ammonia. Ammonia can pass through cell membranes and is converted into ammonium while absorbing protons. This causes the pH to rise, which the cell tries to prevent by balancing the amount of protons through its potassium (K^+) pump. However, this requires more energy from the cell and possibly inhibits certain enzyme reactions. This results in a decrease in biogas production or a sudden increase in VFAs (Rajagopal et al. [2013]; Wirth et al. [2013]; Liu et al. [2019b]). With an increase of these compounds in the effluent, subsequent treatment for a safe and sustainable discharge is needed (Bustillo-Lecompte and Mehrvar [2017]).

To improve the process stability and efficiency of protein-rich wastewater during anaerobic digestion several different pre-treatments have been proposed (Ahn et al. [2001]; Uçkun Kiran et al. [2016]; Bharathiraja et al. [2018]). Within this research project, biological acidification (BA) was chosen due to the fact that no chemicals are dosed, the energy requirements are limited and literature of the effect on proteins is scarce.

2.4 BIOLOGICAL ACIDIFICATION

Biological acidification consists of both hydrolysis and acidogenesis, which both occur in the first phase of a two-stage fermentation process.

Already in 1986 it was deemed necessary to include a two-stage fermentation process for the separation of carbohydrates and proteins (Breure et al. [1986]). This is done to both increase the growth rate of acidogens as well as methanogens, thus preventing inhibition of methanogens by acidogenic products and the resulting low pH. Supplying a separate methane reactor can lead to an increased methane yield and a reduction of effluent COD and solids. Additionally, higher organic loading rates can be applied (Göblös et al. [2008]; Sun et al. [2019]).

Furthermore, carbohydrates should be already fermented to VFAs at a low pH and high rate whereas the fermentation of protein should occur consecutively at neutral pH and high rate. In a subsequent reactor VFAs are then converted into methane (Alexiou [1998]).

Wang et al. [2002] analysed two-stage fermentation of food waste and stated that the first stage of fermentation, especially pre-acidification, plays an important role in the degradation efficiency of the substrate. The main products during pre-acidification were VFAs, the main ones being acetic, butyric and propionic acid.

The most important parameter in the design of a two-phase system is the degree of acidification, which describes the fraction of feed that is present as VFAs. Different degrees, depending on the strength of the wastewater, have been suggested by research groups, such as 20-40% by Lettinga and Hulshoff Pol [1991] and 40-50% by Alexiou et al. [1994].

The hydraulic retention time (HRT), in other words the average residence time of soluble compounds in the bioreactors, is the key parameter for applying different degrees of acidification. Acidogens do not require a long HRT for the hydrolysis and acidogenesis. Furthermore, the applied HRT varies depending on the type and composition of substrate. On the one hand, for slaughterhouse wastewater an HRT of 6.5 to 7 hours was recommended, though yielding no concrete conclusions on its effectiveness (Alexiou [1998]). On the other hand, wastewater from the instant coffee industry degraded most efficiently at an HRT between 6 and 9 hours (Alexiou [1998]).

Although some studies have been conducted on the biological acidification of protein as stated above, no studies report on a holistic approach to degradation, including efficiency and kinetics.

2.5 KNOWLEDGE GAPS

Summarising the identified gaps there are no clear conclusions with regard to the following topics:

1. The impact of the co-digestion of sugar on the anaerobic protein degradation process.

   Besides methane yield and production rate, no other aspects of co-digestion with sugar and protein have been reported in literature. Thus, the effect of co-digestion on proteins has not yet been clearly established. To represent protein-rich wastewater it is further necessary to apply a protein-to-sugar ratio of 1:1, which has not yet been investigated thoroughly.

2. The biological acidification of sugars in the presence of proteins.

   In the analysed literature biological acidification has mostly been investigated in up-scaled systems with real wastewater. A lack of information has thus been identified on the impact on individual compounds.

3. A framework to assess the successful conversion of protein to ammonia.

   Due to the fact that ammonia has only recently been identified as a valuable resource there is a lack of literature on the conversion efficiencies of protein to ammonia. Specifically, a parameter to express the potential of biologically produced ammonia is yet to be developed.

3 RESEARCH QUESTIONS AND HYPOTHESES

This is the first study to, on the one hand, thoroughly analyse the co-digestion of proteins and sugars and, on the other hand, assess biological acidification as a pre-treatment for the anaerobic digestion of a protein and sugar mixture with respect to kinetics and efficiency. Additionally, a parameter to assess biologically produced ammonia is developed in a first attempt.

This report focusses on the combined degradation of sugars and proteins with a focus on kinetics and efficiency.

The main objectives of this thesis are:

"To gain understanding of the co-digestion of sugar and protein under anaerobic, mesophilic conditions, to test biological acidification as pre-treatment for a protein + sugar mixture, and to determine a biological ammonia potential for future applications."

These objectives are reached in such a way that the results contribute to improving process operations of systems for protein-rich wastewater. The main research question to be answered is:

Can the degradability of proteins be improved through the co-digestion with easily degradable carbon sources?

The sub-questions to be answered with regard to the main research question are:

1. What is the impact of sugar on the rate and efficiency of the anaerobic degradation of proteins?

   This question will be answered by testing three different proteins (gelatin, BSA, casein) in combination with glucose and lactose, respectively.

   Based on literature review it is expected that glucose and lactose, as easily degradable carbon sources, do have a positive impact on the degradation of proteins with regard to methane yield and methane production rate. Additionally, if both sugar and protein are consumed equally by the biomass a positive impact on the protein degradation rate and efficiency is expected.

   After the analysis of proteins with sugars in the first step, the sugars in the substrate will be acidified to simulate biological acidification as pre-treatment. This leads to the second research question:

2. What is the impact of pre-acidification on the rate and efficiency of the anaerobic degradation of proteins?

   High degrees of acidification ($\sim$ 25% and 50%) are expected to improve the protein degradation efficiency and rate while yielding a great concentration of volatile fatty acids. The effects on the methane production are dependent on the resulting VFA ratio.

   Lastly, an attempt is made to generalise the production of ammonia from proteins by defining a biological ammonia potential (BAP), which results in the third research question:

3. How can the biological ammonia potential (BAP) of proteins be defined?

   Due to the fact that no standard definition of BAP has been established yet it is not possible to compare with existing literature. Within this research an attempt to come up with a definition will be made.

4 MATERIALS AND METHODS

This chapter introduces the materials and methods that were defined for this research. This entails experimental equipment as well as equations used to, step-by-step, address the stated questions.

4.1 MATERIALS AND METHODS

The granular sludge used for this study was provided by the Corbion site in Gorinchem in South Holland. Corbion produces, among others, chemicals from lactic acid. TS and VS were initially measured to characterise the sludge.

BSA (A7030-100G), gelatin from porcine skin (G2500), α-Lactose monohydrate (L3625-1KG) and D-(+)-Glucose (G8270) were purchased from Sigma Aldrich. Casein (9000-71-9) was purchased from Fisher Scientific and shipped to Biothane in Delft, The Netherlands. Glucose, lactose and BSA are stored at 4°C. Gelatin and casein are stored at room temperature.

Synthetic wastewater was used where proteins and sugars were added to a solution consisting of a buffer and macronutrients. The sample solution consisted of the compounds mentioned in Table 4.1 as well as 20 $mg \cdot L^{-1}$ KH_2PO_4, 15 $mg \cdot L^{-1}$ $MgSO_4 \cdot 7H_2O$, 10 $mg \cdot L^{-1}$ of $CaCl_2$ and 5 $g \cdot L^{-1}$ of $NaHCO_3$ as buffer. The pH was adjusted to 7 using 0.1 M NaOH or HCl for all feeds except for casein feeds for which pH was adjusted to 8 to facilitate the dissolution of the protein.

4.2 EXPERIMENTAL SET-UP

4.2.1 Batch fermentation tests

To test the degradation of proteins under anaerobic conditions a series of batch tests were set up. In a batch set-up there is no in- or outflow, which means that substrate is provided only at the start of the experiment. The experiment was stopped after the cumulative methane production reached a plateau level, which was assessed with a parallel experiment described in Section 4.3. All bottles were set up in duplicates.

Gelatin, BSA and casein were used as model proteins with glucose in combination with gelatin and BSA, and lactose in combination with casein. Table 4.1 shows the composition of substrates as percentages on COD basis. To keep the conditions equal in all batch experiments a COD:N ratio of 8:1 was applied. However, in the mixtures with BSA + glucose and casein + lactose two separate COD:N ratios were investigated. This is denoted as **low N** for a ratio of 16:1 and **high N** for a ratio of 8:1, respectively.

Due to the fact that the conversion factor of COD to protein ($gCOD \cdot gProtein^{-1}$) was not known, a range of dilutions was made to establish a conversion factor from protein to COD. The concentrations used were 0.2, 0.25, 0.5 and 1 $g \cdot L^{-1}$.

Experiments were conducted in glass bottles. For the first batch experiment, bottles of 1 L volume were used for the liquid sampling, whereas 500 mL bottles were used for the BMP test throughout the whole study. From the second batch onwards

Table 4.1: Substrate composition of different mixtures in %COD of proteins and sugars used in each bottle.

Feed name	%Protein	%Sugar
Gel1	100	0
Gel2	50	50
BSA1	100	0
BSA2	50	50
Cas1	100	0
Cas2	50	50

it was decided to also use 500 mL bottles for the liquid sampling bottles to align the conditions in all bottles.

To each bottle, 44 g of granular sludge, 82 mL of $NaHCO_3$ solution and 377 mL of sample solution were added. Blank bottles were prepared in a similar way, the only difference being the addition of 458 mL of buffer solution ($NaHCO_3$).

Initially, all bottles were flushed with oxygen-free gas (70%N_2, 30%CO_2) for 5 minutes and capped tightly with rubber stoppers. The bottles were then placed in an incubator to be maintained at a temperature of 37 °C.

In total 5 liquid samples of 10 mL were taken within a maximum of 150 hours (hours of sampling varied per batch run) because no major changes were expected to occur after this period. The bottles for BMP tests were analysed over a period of 10-30 days depending on the type of substrate used.

4.2.2 Methodology of Acidification

Acidification as a pre-treatment was applied during batch tests as described by Cohen et al. [1985]. Two types of volatile fatty acids (VFAs), namely propionic and acetic acid, were added in a ratio of 3:1 (advised by Biothane) as part of the substrate. The degree of acidification is determined as

$$\%\text{acidification} = \frac{COD_{VFAs}}{tCOD} \times 100(\%) \tag{4.1}$$

and the degrees of acidification tested were 25% and 50%. The composition of substrates based on COD is shown in Table 4.2.

Table 4.2: Substrate composition of pre-treatment mixtures in %COD of proteins, sugars and VFAs used in each bottle.

Feed name	%Protein	%Sugar	%VFAs
BSA3	50	25	25
BSA4	50	0	50
Cas3	50	25	25
Cas4	50	0	50

4.3 BIOMETHANE POTENTIAL TEST (BMP)

A BMP test was performed on all prepared substrates. To validate results, several criteria need to be met for comparison with literature values. These criteria were mostly found in the article of Holliger et al. [2016] unless cited otherwise.

Preparation of the BMP test bottles was identical to the liquid sampling bottles. However, bottles are kept in a water bath at 37 °C and mixed with rotational stainless steel paddles. The test was set up using an Automatic Methane Potential Test

System (AMPTS) II by Bioprocess Control (Sweden). A manual provided by the manufacturer was followed to ensure proper preparation. The substrate to inoculum ratio (SIR) applied was between 0.6:1 and 1:1 $gCOD \cdot gVS^{-1}$.

To validate the test results a positive control is run. In the case of soluble substrates, this control was gelatin. Another aspect to consider was the endogenous gas production of biomass. Therefore, a negative control of the same composition as the blank bottles was prepared as described in Section 4.2.1. A method described by Hafner [2019] was used to calculate the total average methane yield for each substrate. Additionally, the biodegradability was determined. Here, the biodegradability is defined as the methanised COD divided by the total added COD at the start of the experiment. The yield was normalised per kgCOD due to the fact that the theoretical maximum is, on COD basis, the same in all cases ($350 NLCH_4 \cdot kgCOD^{-1}$).

4.4 STOICHIOMETRY OF PROTEIN DEGRADATION

A methodology described by Ramsay and Pullammanappallil [2001] was used to derive the stoichiometry of VFAs produced during anaerobic digestion of protein-rich wastewater.

In a first step, amino acid sequences of the investigated proteins were taken from online protein databases. Then, the chemical formulas ($C_c N_n H_h O_o$) were derived based on the occurrence of each amino acid in the sequence. VFAs can be produced in two distinct ways - through coupled redox-reactions (Stickland) or uncoupled fermentation (single amino acid fermentation). Based on thermodynamics, the more favourable reactions to take place are Stickland reactions, which were chosen as representative for this study. By setting up these reactions for each amino acid, the stoichiometric coefficients in mole/C-mole protein for each VFA ($C_2 - C_5$) can be calculated and verified with measurements during batch tests. The chosen reactions and detailed documentation are presented in Appendix A.2.

4.5 ANALYTICAL METHODS

Liquid samples were used to analyse total nitrogen (TKN) and soluble nitrogen (SKN) according to the Kjeldahl method. The samples were kept in 10 mL sample cups and stored refrigerated at 4°C. The soluble fraction was extracted by centrifuging the samples for 10 minutes at 14000 rpm and subsequent filtering through 0.45 μm membrane filters.

Total COD, soluble COD, as well as ammonium (NH_4-N) were measured using Lange HACH test kits, which were analysed with a spectrophotometer (Lange HACH DR3900).

Protein concentrations were determined via the bicinchoninic acid protein assay of Sigma Aldrich (BCA1-1KT) with a BSA standard solution modified from the Lowry method (Lowry et al. [1994]). The samples were diluted 10 times with demineralised water. 100 μL sample was pipetted into tubes, and filled up to 2.1 mL with the reagent from the kit. The tubes are then left to react in an incubator at 37 °C for 30 minutes. In that time, Cu^{2+}-protein complexes are formed under alkaline conditions, which are then reduced to Cu^{1+}. Afterwards, samples are analysed with a spectrophotometer (Jenway 7315) at 562 nm. Calibration curves are made for each run and each protein (gelatin, BSA, casein), separately. The range for the calibration curves was chosen as described by the manual and covers the concentrations of samples at a dilution of 10.

VFAs were measured using a gas chromatograph (PC) equipped with a flame ionization detector (FID) and a wall coated open tubular (WCOD) fused silica column (25 m $\times$ 0.53 mm). The temperatures of the column and the detector were 140 °C

and 275 °C, respectively. Samples were analysed after fixing 0.5 mL of each sample with an internal standard of 0.5 mL 1-Pentanol. The carrier gas used was nitrogen gas at 5 psi and a flow rate of 28.5 $mL \cdot min^{-1}$.

Gas composition including CH_4, CO_2 and N_2 was determined by a gas chromatograph in the Waterlab of TU Delft (GC, Agilenttech 7809 A). The GC contains an HP-PLOT Molesieve GC column (Agilent 19095P-MS6) of 60 m × 0.53 mm × 200 μm and a thermal conductivity detector (TCD). Helium was used as a carrier gas at 14.8 psi and a flow rate of 23 mL/min. Operation temperature was maintained at 200 °C. For the analysis 10 mL of gas was drawn into a syringe at the sampling point, which was subsequently injected into the GC and analysed.

4.6 CALCULATIONS

4.6.1 Kinetic rates

Hydrolysis of the investigated substrates is often described as a first-order kinetic model

$$S_t = S_0 \cdot e^{-k_{Protein} \cdot t} \tag{4.2}$$

where S_t is the concentration of substrate at time t, S_0 is the start concentration at t = 0, k_{Protein} is the degradation coefficient (t^{-1}) and t is incubation time.

When using the accumulated methane volume to calculate the degradation coefficient the equation is

$$G_t = G_m \cdot (1 - e^{-k_{CH4} \cdot t}) \tag{4.3}$$

where G is the accumulated methane volume at time t, G_m is the maximum achievable methane volume, k_{CH_4} is the degradation coefficient and t is incubation time.

The degradation coefficients were calculated using non-linear curve-fitting tools of equation 4.2 and 4.3 in Matlab and Python 3.6. The obtained values were averaged and presented with deviation. The Pearson product-moment correlation coefficient (R^2) is a measure of the linear correlation between any two variables and was used to determine the goodness of fit for equation 4.2 and 4.3, respectively. The code can be found in Appendix A.3.

4.6.2 Methanised COD

The methanised COD was calculated by the following equation

$$\%M = \frac{\text{COD}_{\text{CH}_4}}{\text{COD}_{\text{initial}}} \cdot 100 \tag{4.4}$$

4.6.3 Free ammonia

Free ammonia (FA) was calculated from the NH_4^+ concentration measured Omil et al. [1995]

$$\text{FA} = \frac{1}{[1 + (k_b \cdot 10^{\text{-pH}}) \cdot \frac{1}{k_w}]} \cdot NH_4^+ \tag{4.5}$$

where k_b and k_w are the dissociation constants for ammonia and water at 37 °C, respectively (1.855 $\times 10^{-5}$ and 2.355 $\times 10^{-14}$ $mol \cdot L^{-1}$).

4.6.4 Mass balances

The COD mass balance was set up based on following equation

$$\%\text{CODbalance} = \frac{\text{COD}_{\text{final}} + \text{COD}_{\text{CH}_4} + \text{COD}_{\text{biomass}}}{\text{COD}_{\text{initial}}} \cdot 100 \tag{4.6}$$

whereas the Nitrogen mass balance was calculated by using the following equation

$$\%\text{Nbalance} = \frac{\text{Protein}_{\text{final}} \cdot f_{\text{N}} + NH_4^+}{\text{SKN}_{\text{initial}}} \cdot 100 \tag{4.7}$$

where f_N is the fraction of nitrogen in protein (%).

4.6.5 Degradation efficiency

COD degradation efficiency was calculated as

$$\%_{COD} = \frac{COD_{initial} - COD_{final}}{COD_{initial}} \tag{4.8}$$

where the COD at the end of the experimental run was deducted from COD at the beginning divided by the initial COD concentration. In the same manner, the protein degradation efficiency was calculated as

$$\%_P = \frac{P_{initial} - P_{final}}{P_{initial}} \tag{4.9}$$

where the protein concentration at the end of the experimental run was deducted from protein at the beginning divided by the initial protein concentration.

4.6.6 Methane yield and biodegradability

The methane yield was calculated by using the following equation

$$\text{Y}_{\text{CH}_4} = \frac{\text{V}_{\text{CH4,S,}i\text{,net}}}{\text{m}_{\text{COD,S,}i}} \tag{4.10}$$

where $\text{V}_{\text{CH4,S,}i\text{,net}}$ is the standardised net volume of CH_4 produced in bottle i with inoculum and substrate at time t, and $\text{m}_{\text{COD,S,}i}$ is the mass of substrate in COD originally added to bottle i.

Biodegradability was calculated according to

$$\%BD = \frac{\text{m}_{\text{COD,CH4,}i}}{\text{m}_{\text{COD,S,}i}} \tag{4.11}$$

where $\text{m}_{\text{COD,CH4,}i}$ is the methane produced in bottle i expressed in COD, whereas $\text{m}_{\text{COD,S,}i}$ refers to the initially dosed COD in bottle i.

4.6.7 Conversion efficiency

To determine the conversion efficiency of nitrogen in protein to NH_4^+ the following formula was used:

$$\%\text{CE} = \frac{NH4^+_{\text{final}} - NH4^+_{\text{initial}}}{\text{SKN} - NH4^+_{\text{initial}}} \tag{4.12}$$

where the numerator represents the amount of NH_4^+ produced and the denominator stands for the concentration of nitrogen excluding the initially present NH_4^+. With this approach only the produced NH_4^+ will be taken into account versus what was initially added to the feed by adding protein and NH_4^+ for a constant COD:N ratio.

4.6.8 Biological ammonia potential

An attempt was made to define a biological ammonia potential (BAP) to develop a parameter for the potential of protein conversion during fermentation. For this, the produced ammonium was calculated as

$$NH_{4,prod}^+ = NH_{4,meas}^+ - NH_{4,blank}^+ - NH_{4,dosed}^+ \tag{4.13}$$

where $NH_{4,blank}^+$ stood for NH_4^+ produced through self-digestion of biomass, $NH_{4,dosed}^+$ was the dosed ammonium at the start of the experiment and $NH_{4,meas}^+$ was the actually measured ammonium. This was then implemented in the following equation

$$\%BAP = \frac{NH_{4,prod}^+}{Protein_{N,dosed}} \cdot 100\% \tag{4.14}$$

and compared to the theoretical ammonia potential, which was the amount of nitrogen present per unit of protein. This was calculated from the grams of N present in each amino acid of the respective protein.

5 RESULTS AND DISCUSSION

This chapter presents the results obtained from the applied methodology. An attempt is made to put values into context with existing knowledge and established explanations.

5.1 SUBSTRATE CHARACTERISATION

To deepen the understanding of utilised substrates in this research an initial characterisation was performed. This included a biogas composition analysis (Appendix B) and the determination of a conversion factor of proteins to COD.

For each protein slightly varying chemical formulas from different sources are reported. Therefore, conversion factors from protein to COD were calculated using varying dilutions. The obtained conversion factor for BSA was 1.47 $gCOD \cdot gProtein^{-1}$, for casein 1.29 $gCOD \cdot gProtein^{-1}$, and for gelatin 1.13 $gCOD \cdot gProtein^{-1}$.

5.2 ANAEROBIC DIGESTION OF GELATIN

This section discusses the results from parameters related to degradation that were measured during the experiment with gelatin, both in the liquid and gas fraction.

5.2.1 Biochemical Analysis

Biomethane potential (BMP) test

The total average yield of methane as well as the curve shape of methane production were used to compare the anaerobic digestion of pure gelatin with gelatin and glucose. The cumulative methane production of several runs with varying runtime is given in Figure 5.1. Due to technical issues it was not possible for some of the feeds to reach a plateau level such as can be observed in Gelatin 1, Gelatin 2, Gelatin 3 and Gelatin 4. However, the values obtained showed a high similarity to the ones obtained during the longer runs. In Table 5.1 the average methane yield as well as the biodegradability of the compounds are shown.

Table 5.1: The average total yield of methane (NL) produced per kilogram of COD and biodegradability of pure gelatin and a gelatin glucose mixture. The BMP yield was calculated with equation 4.10, whereas the formula used for biodegradability is 4.11.

	Averaged BMP yield ($NL_{CH4} \cdot kg_{COD}^{-1}$)	Theoretical methane yield ($NL_{CH4} \cdot kg_{COD}^{-1}$)	Biodegradability
Gelatin (n = 10)	292 ± 5	350	93.4 ± 1.3%
Gelatin + Glucose (n = 4)	320 ± 1	350	93.7 ± 0.3%

From Figure 5.1 it can be seen that the mixture of gelatin and glucose showed an initially faster gas production rate than the pure gelatin batches. This is due

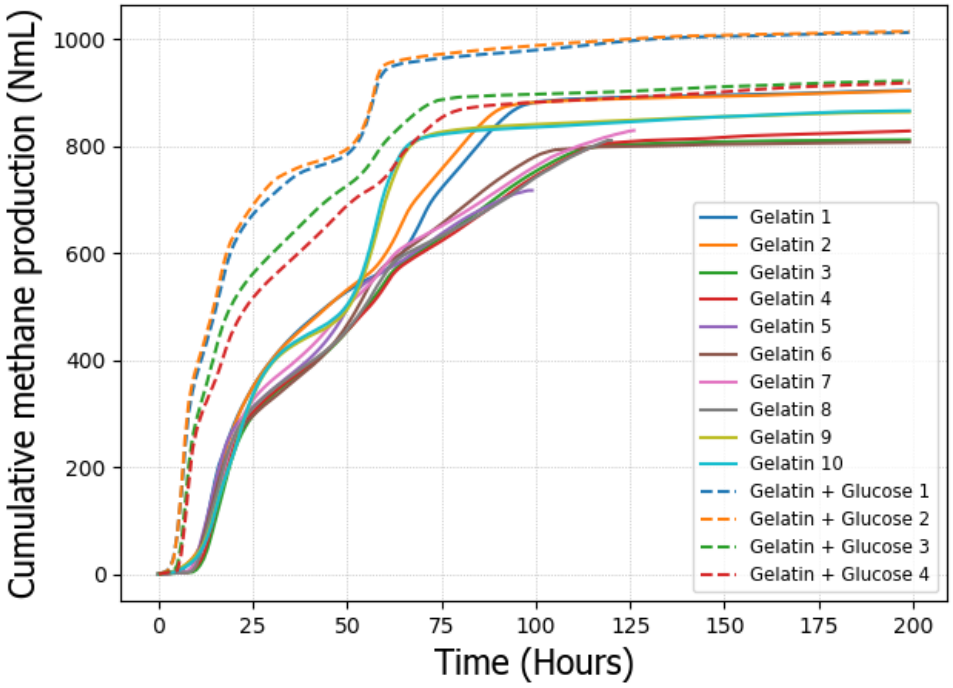

Figure 5.1: Cumulative methane production of gelatin expressed in NmL obtained during the batch anaerobic digestion. Gas production of the negative control (inoculum only) was deducted from the values shown in this graph. The number in the legend refers to the replicates.

to the fact that carbohydrates generally show a higher conversion rate to methane than proteins do (Gavala et al. [2003]). Additionally, if the chemical structures are compared, it becomes apparent that glucose is a much smaller and therefore more easily degradable compound compared to gelatin.

The positive influence of glucose on gelatin for gas production was also reflected in the BMP. As is shown in Table 5.1, the yield of the gelatin and glucose (320 $\pm$ 1 NL_{CH4}/kg_{COD}) mixture was significantly higher than for pure gelatin (292 $\pm$ 5 NL_{CH4}/kg_{COD}). In relation to the theoretical methane yield the gelatin and glucose mixture reached values close to the theoretical maximum (91%) whereas the methane yield of pure gelatin showed a value of 83% of the maximum.

Thus, in general it can be said that even though gelatin by itself already showed a high BMP yield, this was even improved through the co-digestion with glucose.

Degradation efficiency of gelatin

The degradation efficiency is an important operational parameter, and was used in combination with the degradation rate to comment on the efficiency of the anaerobic digestion process. The degradation efficiency of both gelatin and gelatin with glucose are shown in Table 5.2.

Table 5.2: Degradation efficiencies from both COD results and protein measurements. Values for protein were calculated using equation 4.9 whereas for COD equation 4.8 was used.

	Protein degradation (%)	COD degradation (%)
Gelatin	95 $\pm$ 1	86 $\pm$ 1
Gelatin + Glucose	97 $\pm$ 0	92 $\pm$ 1

No significant differences in degradation efficiency between the two feeds were observed. In general, the pure gelatin and the gelatin and glucose mixture showed very high degradation efficiencies with both types of measurements. Furthermore, the degradation efficiency with values from protein measurements were higher than for COD, which is due to the fact that even though protein was already degraded, its intermediate products had not been converted to biogas yet. Additionally, gelatin degradation efficiency is also reported similarly (94 % at pH above 5.5) by another research group (Yu and Fang [2003]).

Conversion efficiency of gelatin to NH_4^+

After the hydrolysis of protein, nitrogen is not yet present in its final form, ammonium, but often still bound in amino acids. Therefore, in order to ensure that intermediate products are completely fermented the conversion efficiency from proteins to ammonium was calculated.

In Table 5.3, the conversion efficiencies of both pure gelatin and the gelatin and glucose mixture are shown.

Table 5.3: Initial and final ammonia concentrations (t = 133 h), soluble Kjeldahl nitrogen and conversion efficiency from gelatin to NH_4^+. Conversion efficiencies were calculated using equation 4.12.

	Initial NH_4^+ (mgNH4-N/L)	Final NH_4^+ (mgNH4-N/L)	SKN (mgN/L)	Conversion efficiency (%)
Gelatin	6	836 ± 8	1137	$74 \pm 1\%$
Gelatin + Glucose	60	455 ± 13	475	$95 \pm 3\%$

Both pure gelatin as well as the mixture showed relatively high conversion efficiencies from protein to ammonia. A significant difference was seen between the values for pure gelatin (74%) and gelatin with glucose (95%). This could be attributed to the difference in dosed protein concentration, which was $8 gCOD \cdot L^{-1}$ for gelatin and only $4 gCOD \cdot L^{-1}$ for gelatin and glucose. In the given time, a lower gelatin concentration meant a higher conversion, whereas a higher concentration meant more ammonia that is produced. However, the COD:N ratio was deliberately kept constant in order to have equal conditions in each batch.

5.2.2 Kinetic analysis

The protein degradation and methane production rates calculated for gelatin and gelatin with glucose are shown in Table 5.4.

Table 5.4: Degradation coefficients calculated from both methane data (equation 4.3) as well as protein concentrations (equation 4.2).

	$k_{Protein}$ (d^{-1})	R^2	k_{CH4} (d^{-1})	R^2
Gelatin	1.13 ± 0.30	0.92	0.42 ± 0.03	0.98
Gelatin + Glucose	1.56 ± 0.12	0.99	0.63 ± 0.12	0.98

In both cases the same trend was observed, namely the higher rate of protein degradation compared to the degradation rate obtained from BMP results. An explanation for this lies in the values used to calculate the kinetic rates. Whereas using concentrations from protein measurements is a direct method to determine the degradation rate and reflects the hydrolysis rate of the process, the rate obtained from BMP data represents the methane production rate, which includes several intermediate steps before methane is produced (Ay et al. [2011]). Furthermore, the hydrolysis rate value obtained for gelatin was slightly elevated to what is reported in literature (Vavilin et al. [2008]). Multiple factors could have an influence on the

difference in values, such as the type of inoculum, macro- or micronutrients added to the solution, type of gelatin, degree of solubilisation, the experimental set-up or the type of curve fitting used.

However, the most important finding of these results was that the protein hydrolysis rate of gelatin and glucose mixture was significantly higher than for pure gelatin. Researchers have been in dissent on this topic, but recently more studies prove the positive effect of sugar on the protein hydrolysis rate (Tommaso et al. [2003]; Elbeshbishy and Nakhla [2012]).

5.2.3 Discussion of results for gelatin trial

The objective for this subpart of the research project was to investigate the impact of glucose on the gelatin degradation in terms of rate and efficiency, as well as the conversion efficiency of gelatin to ammonium. From the results presented in this section it can be concluded that a slight improvement in degradation and bigger improvement in conversion efficiency can be observed when glucose is co-digested with gelatin. This conclusion is valid when applying a COD:N ratio of 8:1. Moreover, the addition of glucose significantly improved the rates observed, for both the protein and methane production rate. An improvement in terms of methane production and protein degradation rate has not yet been reported elsewhere. Conversely, a significant decrease in protein degradation efficiency after the addition of glucose is reported elsewhere. The reason for this is stated as a decrease in the production of proteases (Breure et al. [1986]). However, the main difference between this study and previous studies was the concentration of glucose added, or in other words, the sugar-to-protein ratio. While the ratio applied in this study was 1:1, the lowest ratio reported in other studies is 2:1. In order to confidently use this conclusion for similar experiments it is necessary to measure protease activity to ensure the occurrence of this phenomenon.

On another note, conversion efficiencies of gelatin have not yet been reported in literature. This is, on the one hand, not too relevant for systems in which the removal of COD is the objective. On the other hand, it can be an important parameter in systems where the aim is to optimise ammonia production.

After the experiments with pure gelatin and the gelatin and glucose mixture were executed, both degradation rates and efficiencies observed were very high. Thus, it was concluded that the addition of glucose indeed improves the kinetics and degradation efficiency of protein, and no further trials to test the degradation of gelatin were performed.

5.3 ANAEROBIC DIGESTION OF BOVINE SERUM ALBUMIN

In this section results of several trials with bovine serum albumin (BSA) are presented and discussed. First, the focus lies on the combined digestion of the protein with glucose. Then, the impact of adding VFAs is shown.

5.3.1 Biochemical Analysis

Biomethane potential (BMP) test

During the BMP tests two different combinations with BSA were tested. The cumulative methane production of the tested substrates over time can be seen in Figure 5.2. The shape of the methane production curve is a direct representation of the process stability, e.g., a deviation from the sigmoidal shape could be the result of either process instabilities or gas leakages in the set-up. However, in the case of BSA

there was almost no such deviation visible, thus the anaerobic digestion process in terms of methane production did not seem to be inhibited.

For simplification the values of BSA and BSA + glucose, respectively, were summed up, thus neglecting the differences in nitrogen concentration and COD added because no striking variations in methane production were observed. The calculated yields and biodegradability are shown in Table 5.5.

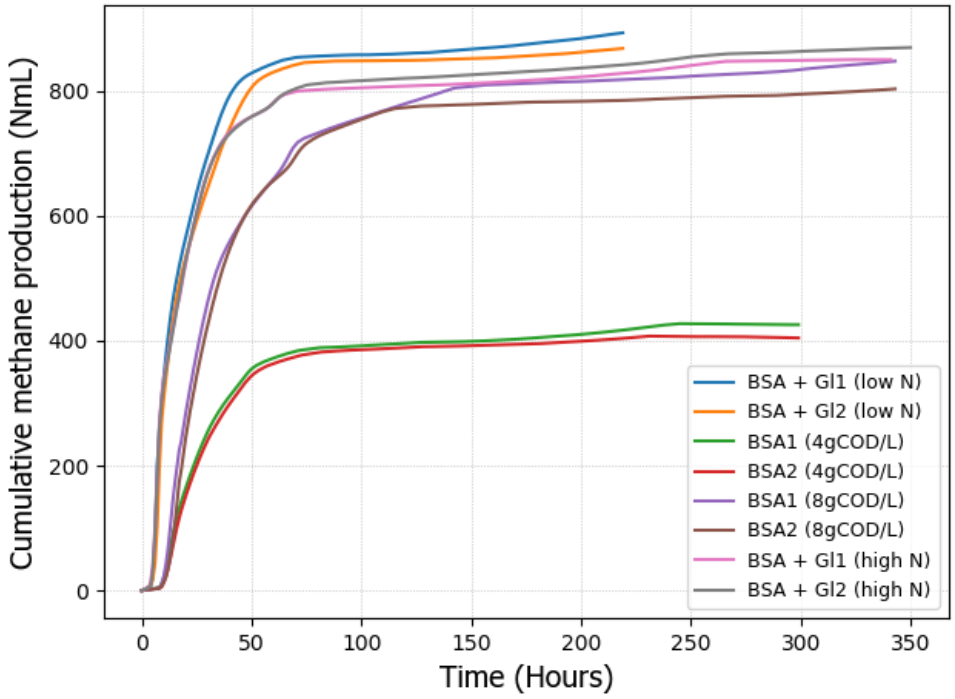

Figure 5.2: Cumulative methane production of BSA expressed in NmL obtained during batch anaerobic digestion. Gas production of the negative control (inoculum only) is deducted from the values shown in this graph.

Table 5.5: The average total yield (equation 4.10) of methane (NL) produced per kilogram of COD and biodegradability (equation 4.11) of pure BSA, a BSA glucose mixture and pure glucose.

	Averaged BMP yield ($NL_{CH4} \cdot kg_{COD}^{-1}$)	Theoretical methane yield ($NL_{CH4} \cdot kg_{COD}^{-1}$)	Biodegradability
BSA (n = 4)	317 ± 5	350	85.2 ± 6.6%
BSA + Glucose (n = 4)	297 ± 6	350	82.2 ± 4.1%
Glucose (n = 2)	293 ± 7	350	95.3 ± 2.1 %

In a study conducted by Elbeshbishy and Nakhla [2012] the methane yield obtained from a BSA:starch ratio of 1:1 is significantly higher to a pure BSA and starch feed. In this case, with BSA and glucose, a significantly higher yield was observed for pure BSA (317 $NL_{CH4} \cdot kgCOD^{-1}$) compared to glucose (293 $NL_{CH4} \cdot kgCOD^{-1}$) and BSA with glucose (297 $NL_{CH4} \cdot kgCOD^{-1}$). A direct comparison is difficult due to the usage of starch instead of glucose. Additionally, it is not specified what type of sludge was used as inoculum for the experiments and the type of macro- and micronutrients used differs from this study. However, it is interesting to see that by using glucose such a difference is observed.

The increased methane yield of protein compared to carbohydrates is also mentioned in another study (Bharathiraja et al. [2018]). Furthermore, a significant increase in biodegradability for glucose (95.3%) was observed compared with BSA and glucose (82.2%). This degree of biodegradability for glucose is expected due to its easily degradable nature.

Degradation efficiency of BSA

In the case of BSA two different concentrations, namely $4 gCOD \cdot L^{-1}$ and $8 gCOD \cdot L^{-1}$, were investigated in addition to the comparison between a high concentration of easily accessible nitrogen in the form of NH_4^+ with a low concentration. The degradation efficiencies are stated in Table 5.6.

Table 5.6: Degradation efficiencies from both COD results (equation 4.8) and protein measurements (equation 4.9) for BSA.

	Protein degradation (%)	COD degradation (%)
BSA (4gCOD/L)	82 ± 1	77 ± 1
BSA (8gCOD/L)	82 ± 1	88 ± 0
BSA + Glucose (low N)	83 ± 1	87 ± 1
BSA + Glucose (high N)	96 ± 1	94 ± 1

The first remarkable observation is that, based on the concentration, there was no difference in protein degradation efficiency of BSA at 4 and $8 gCOD \cdot L^{-1}$. However, looking into the COD removal the efficiency values varied significantly. This can be explained by the duration of experiments. While both BSA at $8 gCOD \cdot L^{-1}$ and the BSA and glucose mixture with a high nitrogen concentration were run for a total of 134 hours, the other two feeds (BSA at $4 gCOD \cdot L^{-1}$) and BSA + glucose with low nitrogen concentration) were only run for 72 hours. By doubling the time and the concentration of BSA the same efficiency can be observed, which could imply that there is no inhibition of the increased BSA concentration. However, another experimental run with the same timespan is required to verify this.

In contrast, the COD degradation efficiency was lower for the $4 gCOD \cdot L^{-1}$ feed. This indicates that while the protein is already degraded, there is still a distinct concentration of intermediate products, such as amino acids or VFAs, detectable, which would require more time to be degraded.

Another implication of these results was that there seems to be no negative impact in protein degradation imposed on BSA by glucose, due to the fact that there is no significant change in degradation efficiency.

Lastly, from these results it seemed as if a higher concentration of easily accessible nitrogen improved the degradation efficiency of both protein and COD significantly. Nevertheless, as already mentioned in this section, there was a remarkable difference in run time between both experiments, which has an influence on the values of degradation efficiency. Therefore, no concrete conclusions can be made on the influence of the increased nitrogen concentration.

Conversion efficiency of BSA to NH_4^+

The conversion efficiencies (CEs) of BSA and BSA with glucose are shown in Table 5.7.

On the one hand, if the pure BSA is considered, no significant difference was observed between the two feeds of different concentrations. This is also reflected in the degradation efficiencies shown in Table 5.6.

On the other hand, a significant difference was detected for the BSA and glucose feeds with different initial nitrogen concentrations. The reason for this lies in the way that the conversion efficiency is calculated. The initial dosage of nitrogen was

Table 5.7: Initial and final NH_4^+ concentrations (t = 133 h) and conversion efficiency (equation 4.12) from BSA to NH_4^+. (*Note: Run time of the experiment was only 72 hours compared to 133 hours for the other two feeds.)

	Initial NH_4^+ (mgNH4-N/L)	Final NH_4^+ (mgNH4-N/L)	SKN (mgN/L)	Conversion efficiency
BSA* (4gCOD/L)	0	284 ± 3	312	$91 \pm 1\%$
BSA (8gCOD/L)	7	647 ± 7	690	$94 \pm 3\%$
BSA + Glucose* (low N)	7	238 ± 3	278	$85 \pm 1\%$
BSA + Glucose (high N)	110	289 ± 13	396	$68 \pm 2\%$

elevated more than 15 times compared to the low nitrogen feed whereas the final NH_4^+ concentration did not differ greatly between the two feeds.

Even though the degradation efficiencies of BSA and BSA and glucose, as reported in Table 5.6, did not differ significantly, the conversion efficiencies did show different results. One reason for this could be the type of measurement used to determine the ammonia and protein concentrations. Since both methods are photospectrometric the interferences from other substances cannot be excluded. It is well known that especially the bicinchoninic acid (BCA) method is prone to show interferences with glucose, which skews results. As opposed to this, it is not precisely known which other compounds could cause a reaction with the provided HACH kits.

Furthermore, for the nitrogen mass balance for BSA and glucose there was a discrepancy of the individually measured soluble compounds versus the total soluble Kjeldahl nitrogen for both the low N (118%) as well as the high N (91%).

5.3.2 Kinetic analysis

Both the hydrolysis rates and methane production rates obtained for BSA and BSA with glucose are shown in Table 5.8.

Table 5.8: BSA degradation (equation 4.2) and methane production (equation 4.3) coefficients.

	$k_{Protein}$ (d^{-1})	R^2	k_{CH4} (d^{-1})	R^2
BSA (4gCOD/L)	0.57 ± 0.02	0.95	0.69 ± 0.02	0.98
BSA (8gCOD/L)	0.81 ± 0.06	0.93	0.44 ± 0.23	0.97
BSA + Glucose (low N)	0.68 ± 0.02	0.98	1.07 ± 0.04	0.99
BSA + Glucose (high N)	1.09 ± 0.20	0.97	1.01 ± 0.57	0.99

Both BSA feeds showed degradation rates that are in the range of what has been reported in other studies (Tommaso et al. [2003]). We can see that the feed with a higher protein concentration (8 $gCOD \cdot L^{-1}$) showed a significantly higher degradation rate compared to the feed with 4 $gCOD \cdot L^{-1}$. This was expected as an increase in concentration increases the reaction rate. Since this is a microbiological process an increase in the degradation rate also indicates that the biomass does not show any inhibitory behaviour. However, if the methane production rates are also taken into account, it seems that the lower concentrated feed showed a higher production rate of methane. The difference was not significant because the deviation in methane production rate for the higher concentrated feed is quite elevated (53%). Therefore, no concrete conclusions could be made comparing the two concentrations of BSA from this aspect.

Contrarily, the same trend in all feeds could be observed, which is the increase in rates when glucose was added. It becomes apparent that glucose had a positive

impact on the methane production rate, which comes from the fact that glucose is an easily biodegradable compound. However, according to the results also the protein degradation rate increased with the addition of glucose. This would mean that both substrates, BSA and glucose, were consumed and converted simultaneously by the present microorganisms without retardation.

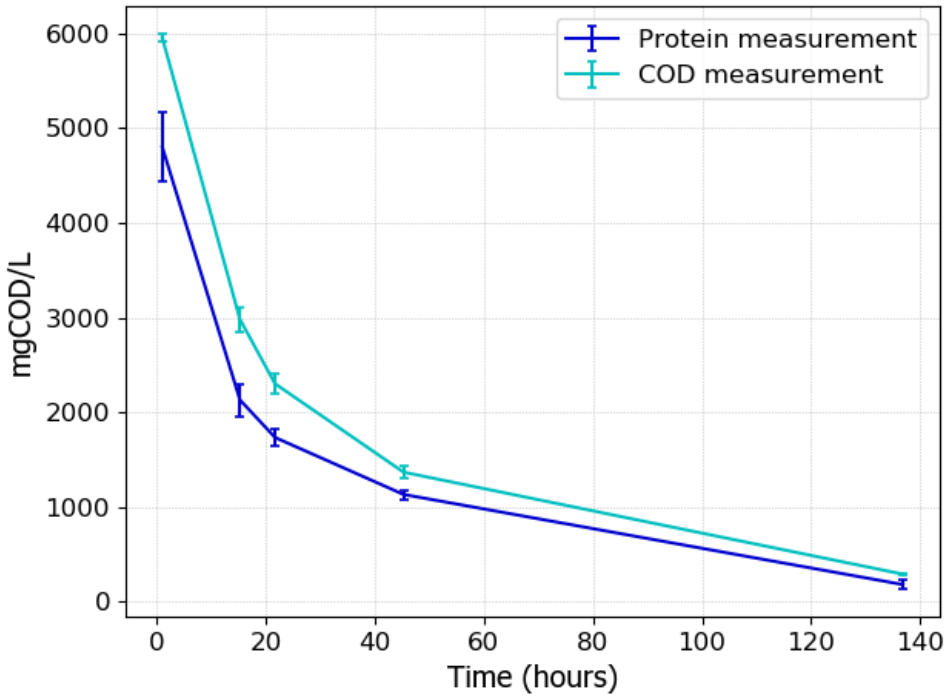

Figure 5.3: BSA and glucose concentrations over time. Protein (dark blue) is measured with the BCA kit and converted to COD via the conversion factor defined in Section 5.1, and COD (turquoise) concentrations are both expressed in $mgCOD \cdot L^{-1}$.

5.3.3 Impact of glucose on BSA

In Figure 5.3 the progressing degradation of BSA and glucose is depicted with BSA measured as both COD and protein. The distance between the data points represents the difference between total COD and COD of protein. This difference is formed by glucose and intermediate products in the feed solution. Here, it becomes more clear that the anaerobic digestion of glucose and intermediate products occurred without negative consequences for the protein degradation, considering that the area in between the two data sets shrank noticeably.

Similar to gelatin, the objective for BSA was to analyse the influence of glucose on the BSA degradation with regard to the rate, efficiency and conversion to NH_4^+. If, on the one hand, all results reported in this section are taken into consideration it can be concluded that the addition of glucose increased the protein degradation and methane production rate considerably. On the other hand, no significant changes were observed for the degradation efficiencies except for a significant increase if additional nitrogen, in the form of NH_4^+, is added. Furthermore, a lower conversion efficiency was detected if glucose was added to BSA. This could be due to interferences based on the methods chosen for this research project and therefore no definite conclusions could be drawn.

5.3.4 Simulated acidification of BSA

After the addition of glucose two more scenarios were investigated:

1. Total acidification of glucose
2. Partial acidification of glucose

In both cases glucose was replaced with VFAs. In the case of total acidification 50% of the feed was added as BSA and 50% as VFAs, whereas partial acidification meant a composition of 50% BSA, 25% glucose and 25% VFAs. The ratio of VFAs (acetate + propionate) was established by using results from earlier trials executed at Biothane. In this section a comparison of both scenarios is made based on process stability with regard to methane production and free ammonia concentration as well as the protein degradation rate and conversion efficiency.

Process stability

In this section, an attempt was made to show a more direct connection between the methane production and VFA concentration. In Figure 5.4 two subplots are shown; Figure 5.4a shows the methane production rate for different degrees of acidification and Figure 5.4b shows the VFA concentrations of the same degrees of acidification.

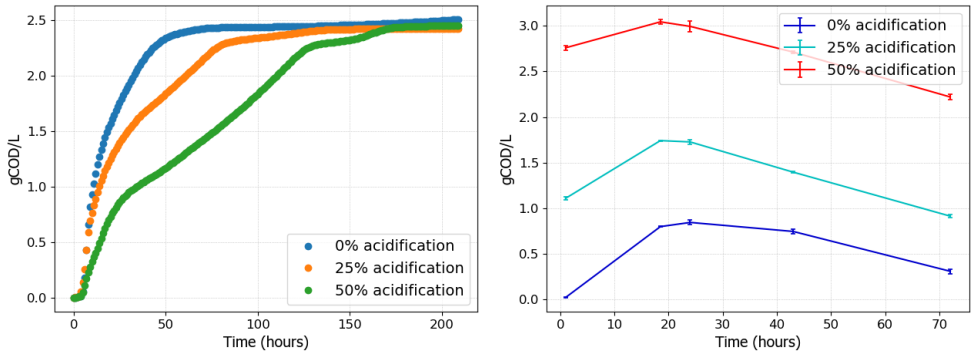

(a) Averaged methane production over time of BSA with glucose (blue), BSA + glucose + VFAs (orange) and BSA with VFAs (green)

(b) VFA concentrations in COD equivalents of all degrees of acidification: 0% (blue), 25% (turquoise) and 50% (red)

Figure 5.4: The effect of acidification showed to have a significant impact on the methane production (left). VFA concentrations of up to 3gCOD/L were reported for 50% acidification (right).

It is clearly visible that the highest concentration of VFAs correlated with the highest decrease in methane production over time whereas a less drastic reduction was observed for 25% acidification. Nevertheless, a concentration of VFAs of $3gCOD \cdot L^{-1}$, as measured at 50% acidification, did not necessarily mean that the system's performance was lowered. A better indicator for this is the propionate concentration. Figure 5.5 shows both the propionate concentration (Figure 5.5a) as well as the free ammonia concentration (Figure 5.5b).

Recently, two research groups (Li et al. [2017]; Bonk et al. [2018]) reported on the connection between free ammonia during anaerobic digestion in combination with elevated propionate concentrations. It is believed that a free ammonia concentration above 40 $mgNH_3 - N \cdot L^{-1}$ can already have detrimental effects on the participating microorganisms. In this research, concentrations up to 119 $mgNH_3 - N \cdot L^{-1}$ for 25% acidification and 105 $mgNH_3 - N \cdot L^{-1}$ for 50% acidification were measured (Figure 5.5b), which was almost 3-fold the concentration of inhibition, indicating that retarded degradation of propionate was likely.

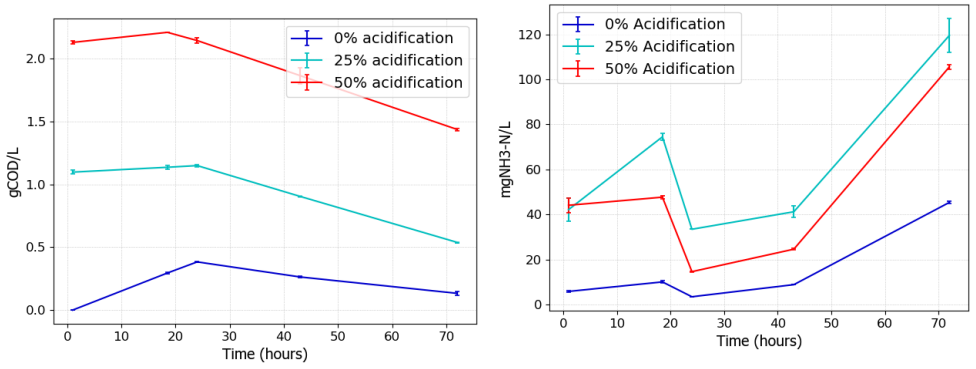

(a) Propionate concentrations in COD equivalents for 0% (blue), 25% (turquoise) and 50% (red) acidification

(b) Free ammonia concentrations in mgNH3-N/L of 0% (blue), 25% (turquoise) and 50% (red) acidification. Free ammonia was calculated according to equation 4.5.

Figure 5.5: The increase in both propionate (left) and free ammonia (right) might have an impact on the lowered methane production rate.

BSA degradation and conversion efficiencies and rates

In both acidification trials protein concentrations were measured over the course of 72 hours. Table 5.9 shows the degradation coefficients for both methane production and protein degradation. In Table 5.10 degradation efficiencies for both acidification trials are shown.

Table 5.9: BSA degradation (equation 4.2) and methane production (equation 4.3) coefficients for both acidification trials.

	$k_{Protein}$ (d^{-1})	R^2	k_{CH4} (d^{-1})	R^2
BSA (50% acidification)	0.58 ± 0.02	0.99	0.33 ± 0.03	0.99
BSA (25% acidification)	0.7 ± 0.01	0.98	0.73 ± 0.01	0.99

Table 5.10: BSA degradation efficiencies (equation 4.9) expressed in protein (second column) as well as COD (4.8) (third column) for both acidification trials.

	Protein degradation (%)	COD degradation (%)
BSA (50% acidification)	82 ± 0 %	56 ± 1%
BSA (25% acidification)	80 ± 1%	78 ± 0%

Looking into the protein degradation coefficients it is clear that if VFAs made up 50% of the substrate there was no improvement of protein degradation observable (0.58 d^{-1}), compared to the pure BSA feed where the obtained degradation rate was 0.57 d^{-1}. This might, on the one hand, indicate that there was no noticeable impact of the propionate or free ammonia concentration on the hydrolysing biomass. On the other hand, the methane production rate was severely decreased (0.33 d^{-1}). This was already shown visually in Figure 5.4a, however, the calculated values give additional support to this assumption.

In addition, we could see that a substrate consisting of 25% VFAs generally showed higher rates for both protein hydrolysis and methane production compared to the 50% acidified feed. If the propionate and free ammonia concentrations are also considered, this implies that, even though the free ammonia concentration of this feed was more elevated than in the 50% acidification trial, the propionate concentration was more impactful with regard to process stability than the free ammonia concentration. On a bigger scale this means that, at mesophilic conditions, the system is more operable at an elevated pH than at an increased propionate concentration.

Further, a similar trend was observed for the degradation efficiencies. In the case of 50% acidification there was virtually no difference to the pure BSA feed (82.4%). Nevertheless, the COD degradation efficiency was significantly decreased, owing to the accumulation of intermediate products, such as propionate, in particular. At the same time, a smoother process was observed for the 25% acidification trial where only a slight difference of 2.4% between the protein and COD degradation was detected.

Lastly, the conversion efficiencies are shown in Table 5.11.

Table 5.11: Initial and final NH_4^+ concentrations (t = 72 h), SKN and conversion efficiency (equation 4.12) from BSA to NH_4^+ for both acidification trials.

	Initial NH_4^+ (mgNH4-N/L)	Final NH_4^+ (mgNH4-N/L)	SKN (mgN/L)	Conversion efficiency
BSA (50% acidif.)	2	261 ± 13	388	85 ± 10%
BSA (25% acidif.)	4	270 ± 9	409	90 ± 1

From the numbers depicted in Table 5.11 no significant difference in conversion efficiencies was observed, owing to the high deviation of the 50% acidified feed. Concluding from this data, it becomes apparent that the different degrees of acidification did not influence the conversion of BSA to ammonium.

5.3.5 Discussion for BSA

The objective for this part of the research project was to, in a first step, analyse the impact of glucose on the BSA degradation and, subsequently, to assess the applicability of increasing the VFA concentration, here called simulated acidification, to improve the protein degradation.

A statistical difference was observed after the addition of glucose to pure BSA in both protein degradation as well as methane production rates. However, no statistical difference was observed in terms of biodegradability or degradation efficiency. Additional nitrogen dosing, however, resulted in a significant increase in degradation efficiency, which was difficult to compare due to the different run times of the batch experiment. Therefore, no clear conclusions could be made based on the difference in nitrogen concentration.

Tommaso et al. [2003] observed a decrease in the protein degradation rate after addition of carbohydrates, and even more so after addition of lipids. The carbohydrates used in this research consisted of starch and glucose. The reason for the decrease in degradation rate could therefore be the mixture of carbohydrates. It is generally known that starch first has to be broken down before glucose is formed. A starch molecule consists of several glucose units that are joined together by glycosidic bonds. Microorganisms then have to excrete more enzymes in order to break down these bonds before the carbon source is accessible, which could be a reason of retardation in anaerobic digestion reported by this research group. However, they state that the most stable process was achieved with the mixture of BSA and carbohydrates.

As opposed to this, Elbeshbishy and Nakhla [2012] reported in 2012 that the degradation of BSA is accelerated if starch is added. With a starch:BSA ratio of 1:1 an increased degradation rate of 0.84 d^{-1} was achieved.

Our research project adds to these conflicting views and it was concluded that glucose indeed improves the BSA degradation rates.

Small-scale batch trials of acidification with the applied methodology have only been reported for glucose (Cohen et al. [1985]) where a significant increase in the specific COD-conversion rates of the sludge was reported. However, it must be mentioned that the maximum degree of acidification applied in their research was 13% compared to the 25% and 50% applied in this research.

Furthermore, the most crucial aspect of pre-acidification was the VFA ratio. It is not very straightforward to pinpoint which type of VFA will be produced as this is dependent on the type of feed (Vidra and Németh [2018]). Hejnfelt and Angelidaki [2009] determined a protein:carbohydrates ratio of roughly 18:1 for blood and 0.35:1 for raw waste, which is a mixture of meat, fat and bones. If the only protein that is considered is BSA, a ratio above 1 would be beneficial to overcome inhibition by propionate, due to the fact that mostly acetate (90 $mgCOD \cdot L^{-1}$) and iso-butyrate (142 $mgCOD \cdot L^{-1}$) are produced. Even though the degradation of iso-butyrate and propionate are both thermodynamically unfavourable, the energy required is lower (48.1 $kJ \cdot mol^{-1}$) than for propionate (76.1 $kJ \cdot mol^{-1}$) (van Lier et al. [2008]). If glucose is also taken into the equation the process will become less stable since the acetate:propionate ratio rises to 1:5 for this mixture (all VFA profiles are found in appendix B). Nonetheless, this is just an indication and the exact feed needs to be analysed in order to give a thorough recommendation.

5.4 ANAEROBIC DIGESTION OF CASEIN

In this section results of several trials with casein are presented and discussed. First, the focus lies on the co-digestion of casein with lactose. Then, the impact of adding VFAs on degradation is shown.

5.4.1 Biochemical Analysis

Biomethane potential (BMP) test

The cumulative methane production can be seen in Figure 5.6. BMPs were calculated and displayed in Table 5.12. As can be seen in Figure 5.6 the difference between a high nitrogen and low nitrogen concentration was negligible, thus the BMP yield was averaged in this case. The BMP of casein was low with a high deviation, which was due to the sudden stop of one of the replicates after 64 hours. If this value is neglected a yield of roughly 300 NL_{CH4}/kg_{COD} was obtained. This also reflected in the biodegradability, which showed a high deviation relative to the other feeds.

Table 5.12: The average total yield (equation 4.10) of methane (NL) produced per kilogram of COD and biodegradability (equation 4.11) of pure casein, a casein lactose mixture and pure lactose. (*Note: The various casein and lactose trials were averaged to one BMP yield and biodegradability value.)

	Averaged BMP yield (NL_{CH4}/kg_{COD})	Theoretical methane yield (NL_{CH4}/kg_{COD})	Biodegradability
Casein (4gCOD/L) (n = 2)	240 ± 60	350	84.3 ± 15.5%
Casein + Lactose* (n = 4)	294 ± 7	350	90.8 ± 3.5%
Lactose (n = 2)	283 ± 2	350	87.4 ± 0.2 %

No statistical difference in BMP yield was observed if lactose was added to casein. Lactose is considered a more easily degradable compound, but in terms of methane production the same trend as for glucose was observed, namely that proteins generally showed a higher yield than carbohydrates. In terms of biodegradability, it was observed that after the addition of lactose an increase in biodegradability occurred, which could also be attributed to the simpler structure of lactose.

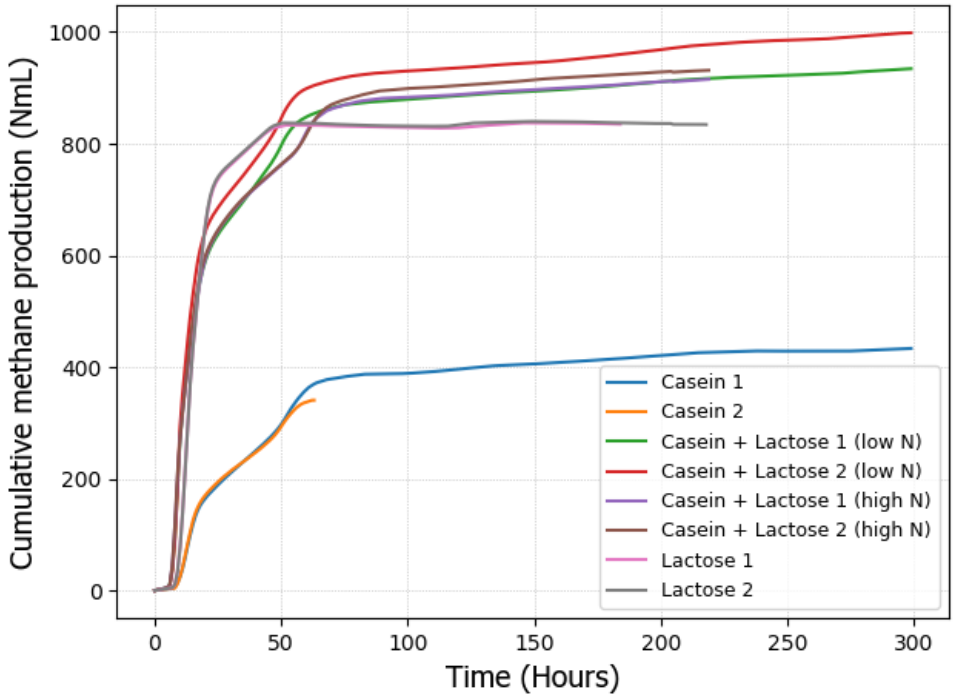

Figure 5.6: Cumulative methane production of casein in NmL during the batch anaerobic digestion. Gas production of the negative control (inoculum only) is deducted from the values shown in this graph.

Degradation efficiency of casein

Just as for BSA, in the case of casein two separate concentrations ($4 gCOD \cdot L^{-1}$ and $8 gCOD \cdot L^{-1}$) as well as a high and low COD:N ratio for the casein and lactose mixture were investigated. The values are displayed in Table 5.13.

Table 5.13: Degradation efficiencies from both COD results (equation 4.8) and protein measurements (equation 4.9) for casein. The run time of both experiments was 133 hours for $8 gCOD \cdot L^{-1}$ casein and the casein and lactose concentration with high dosage of nitrogen and 142 hours for the other two, respectively.

	Protein degradation (%)	COD degradation (%)
Casein (4gCOD/L)	82 ± 1	84 ± 2
Casein (8gCOD/L)	73 ± 2	71 ± 1
Casein + Lactose (low N)	81 ± 2	89 ± 3
Casein + Lactose (high N)	78 ± 2	88 ± 0

Based on these values, a doubling of concentration for pure casein resulted in a significant decrease in degradation efficiency. However, a concentration of $8 gCOD \cdot L^{-1}$ of pure casein is rarely the case, even in protein-rich wastewater (Lin et al. [2017]). Additionally, no significant differences between the COD and protein degradation efficiencies was observed, which means that at the end of the experiment all intermediate products were either converted into biogas or their concentration was negligible.

According to the results, the addition of nitrogen in the form of NH_4^+ had no significant influence on the degradation efficiency of casein and lactose in terms of protein measurements. Moreover, no significant differences were observed for the COD measurements. However, when protein and COD measurements were compared, a significant difference was observed between the two. The increased COD conversion was attributed to lactose.

On another note, there seemed to be neither improvement nor impairment in the degradation efficiency after the addition of lactose. Similar studies such as for gelatin or BSA have not yet been reported for casein. However, the results for both gelatin and BSA showed the same trend: no decline in degradation efficiency was observed after the addition of an additional carbon-source in the form of sugar.

5.4.2 Kinetic analysis

Both the hydrolyis rates as well as methane production rates obtained for casein and casein with lactose are shown in Table 5.8.

Table 5.14: Casein degradation (equation 4.2) and methane production (equation 4.3) coefficients.

	$k_{Protein}$ (d^{-1})	R^2	k_{CH4} (d^{-1})	R^2
Casein (4gCOD/L)	0.18 ± 0.04	0.92	0.50 ± 0.01	0.99
Casein (8gCOD/L)	0.98 ± 0.02	0.75	-	-
Casein + Lactose (low N)	0.13 ± 0.02	0.86	0.79 ± 0.1	0.97
Casein + Lactose (high N)	0.84 ± 0.08	0.69	0.68 ± 0.01	0.96

At a first glance the kinetic rates for the different concentrations of casein varied tremendously. The increased kinetic rate for casein with $8gCOD \cdot L^{-1}$ can be explained by the substrate concentration. During all the trials with casein the protein concentration never decreased below $1290mgCOD \cdot L^{-1}$, which leads to the assumption that there is some inert fraction of casein that would require more time than $\sim$ 140 hours to degrade. Since the $8gCOD \cdot L^{-1}$substrate showed similar concentrations as the $4gCOD \cdot L^{-1}$ substrate at the end of the run, such an increased degradation rate seems logical. Moreover, no methane data is available for the casein at a concentration of $8gCOD \cdot L^{-1}$ due to a leakage in one of the bottles, which therefore showed a high deviation and is deemed unreliable.

The same explanation applies for the comparison of both casein and lactose feeds. The initial concentration of the high nitrogen concentration feed was $1gCOD \cdot L^{-1}$ higher than for the low nitrogen concentration feed. At the end of the experiment protein concentrations for high and low nitrogen feeds were 1178 and 1103 $mgCOD \cdot L^{-1}$, respectively. This difference in starting concentrations and virtually identical end concentrations caused a significant difference in the obtained rates. A similar trend was observed for BSA and glucose, where the increased nitrogen concentration improved the protein degradation, which could also occur in the case of casein and lactose.

Next, there was no significant difference observed between the degradation rates of casein and casein with lactose at a low nitrogen concentration. Considering that the fit for those two feeds was the highest (0.92 and 0.86, respectively) they were also deemed most reliable. However, when the methane production rate was considered there was a significant increase detectable with the addition of lactose, which, together with the obtained methane yields in section 5.4.1, showed that lactose indeed had a positive impact on the methane production rate and yield while not disturbing the degradation of casein.

It was difficult to compare these values with literature since there are no studies known that investigated the kinetics of casein degradation, or the interaction of casein with lactose. Overall, the protein kinetics obtained are similar of what is reported elsewhere ($\sim$ 0.25 d^{-1} for protein) (Siegrist et al. [2002]).

5.4.3 Simulated acidification of casein

Just as for BSA, two cases, total acidification and partial acidification, were investigated for casein.

In both cases lactose was (partially) replaced with VFAs. The ratio of VFAs (acetate + propionate) was established by using results from earlier trials executed at Biothane. In this section a comparison of both scenarios was made based on process stability with regard to methane production and free ammonia concentration, as well as the protein degradation rate and conversion efficiency.

Process stability

The methane production rate and VFA concentration give a good indication for process stability. As can be seen in Figure 5.7a an increase in VFA as part of the substrate resulted in a tremendous decrease in methane production rate. Compared to 0% (45h) and 25% (80h) acidification, the conversion of $2gCOD \cdot L^{-1}$ at 50% acidification was reached after 100 hours runtime, which is the threshold for a biodegradability of 80%.

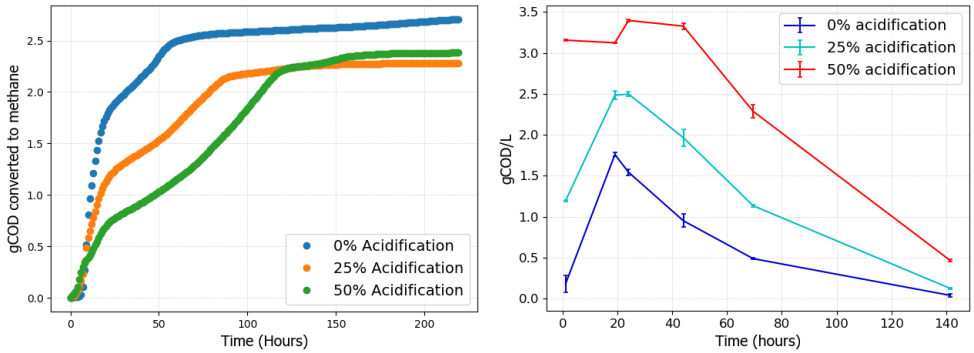

(a) Averaged methane production over time of casein with lactose (blue), casein + lactose + VFAs (orange) and casein with VFAs (green)

(b) VFA concentrations in COD equivalents of all degrees of acidification: 0% (blue), 25% (turquoise) and 50% (red)

Figure 5.7: The effect of acidification showed to have a significant impact on the methane production (left). VFA concentrations of up to $3gCOD \cdot L^{-1}$ were reported for 50% acidification (right).

Besides, VFA concentrations of up to $3gCOD \cdot L^{-1}$ were observed. As already stated for BSA, the total VFA concentration does not give any indication on process instability in the reported range. The specific volatile fatty acids have to be measured in order to comment properly on an imbalance. It was further observed that there was an initial production phase that lasted for roughly 23 hours before a decrease in concentration was measured. This initial increase meant that the more complex substrate, such as casein and lactose, was being converted.

In Figure 5.8 both the propionate (Figure 5.8a) and free ammonia concentration (Figure 5.8b) are shown. Similar values as during the BSA trials were reached, where an inhibition due to the interplay of free ammonia and propionate concentration was suggested. Therefore, the same explanation is expected to be valid in the case of casein. However, due to the longer runtime it was seen that the propionate concentration diminished after $\sim$ 70 hours, which was not observed as distinctively during the BSA trials. This can, on the one hand, be explained by the VFA production from both proteins. During the BSA trials a higher propionate than acetate production was observed for the BSA and glucose mixture. On the other hand, lactose itself is converted into galactose and then glucose, which then has multiple pathways based on the dominant microorganisms present in the biomass. Casein, however, is first disassembled into its amino acids, which are then preferably following the Stickland reaction to be converted into VFAs (Ramsay and Pullammanappallil [2001]; Hassan and Nelson [2012]). In the same study (done by Ramsay and Pullammanappallil [2001]) it was determined that the VFAs produced from casein are acetic acid, butyric acid, valeric acid and eventually propionic acid, in this or-

der. That means that the applied acetate:propionate ratio was not representative of casein or lactose acidification.

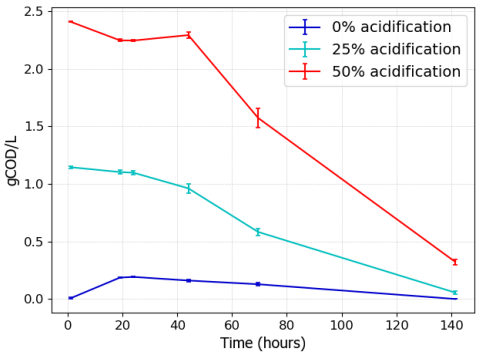

(a) Propionate concentrations in COD equivalents for 0% (blue), 25% (turquoise) and 50% (red) acidification

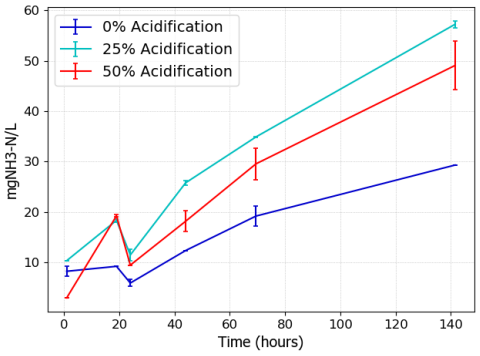

(b) Free ammonia concentrations in mgNH3-N/L of 0% (blue), 25% (turquoise) and 50% (red) acidification. Free ammonia was calculated using equation 4.5.

Figure 5.8: The increase in both propionate (left) and free ammonia (right) might have an impact on the lowered methane production rate.

Moreover, lower free ammonia concentrations were observed during the casein trials, which had to do with the pH in the batch. The pH during BSA trials generally was roughly 0.4 higher than during the casein trials, except for the protein and sugar mixture. The pH measurements of the rest of the trials are listed in appendix B.3.

Summarising the obtained results, it was found that high propionate concentrations were the cause for a decrease in the methane production rate. However, the inhibition was overcome faster due to the low propionate production by casein and lactose themselves, as well as relatively low free ammonia concentrations.

Casein degradation efficiencies and rates

In both acidification trials protein concentrations were measured over the course of 142 hours. Table 5.15 shows the degradation rates as well as methane production rates for the acidification trials. Table 5.16 shows the degradation efficiencies for both protein and COD measurements.

Table 5.15: Casein degradation (equation 4.2) and methane production (equation 4.3) coefficients for both acidification trials.

	$k_{Protein}$ (d^{-1})	R^2	k_{CH4} (d^{-1})	R^2
Casein (50% acidification)	0.16 ± 0.03	0.57	0.33 ± 0.02	0.98
Casein (25% acidification)	0.16 ± 0.01	0.67	0.60 ± 0.03	0.99

Table 5.16: Casein degradation efficiencies expressed in protein (second column; equation 4.9) as well as COD (third column; equation 4.8) for both acidification trials.

	Protein degradation (%)	COD degradation (%)
Casein (50% acidification)	68 ± 1%	87 ± 0%
Casein (25% acidification)	75 ± 0%	87 ± 1%

Both casein degradation rates showed no significant difference. In comparison with the pure protein as well as casein and lactose feeds (0.18 and 0.13 d^{-1}, respectively) there was also no significant difference detectable, which indicates that the addition of VFAs as substrate, even at 50%, did not significantly inhibit the degradation of casein. However, the fit for both values was poor, thus no strong conclusions could be drawn from the protein hydrolysis rates of the acidification batches.

Nevertheless, the methane production rates differed significantly. Acidification of 50% resulted in a distinct decrease, which is also observable in Figure 5.7a. Compared with the pure casein and casein with lactose feed, the casein and lactose mixture showed the highest methane production rate of all (0.79 d^{-1}, Table 5.14), whereas the 25% acidification trial yielded the second highest production rate (0.60 d^{-1}, Table 5.15).

Looking into the degradation efficiencies, we observed a significantly higher efficiency of 75% for the 25% acidification trial compared to 68 $\pm$ 1% for 50% acidification. One of the reasons for this discrepancy in efficiencies, which will also be discussed in the following subsection, could be the hydrophobic nature of casein and its tendency to precipitate at a lower pH. At the start of the experiment COD measurements were taken to quantify the amount that was added to the bottles. Due to the adding of VFAs, casein precipitated, even though the pH was kept at 7.5 with the buffer solution. In total, $8 gCOD \cdot L^{-1}$ were dosed in the 50% acidified solution but only $6.2 gCOD \cdot L^{-1}$ could be measured. This means that $1.8 gCOD \cdot L^{-1}$ ($>$ 20% of the dosed concentration) could initially not be measured because of precipitation of the feed. The precipitation flocs are shown in Figure 5.9. A similar scenario was also observed for the 25% acidified feed, where $1.7 gCOD \cdot L^{-1}$ was initially "lost".

Also, both acidification trials (68 $\pm$ 1% for 25% and 75 $\pm$ 0% for 50%) showed significant differences to the pure casein and casein and lactose trials (82 $\pm$ 1% and 81 $\pm$ 2%, respectively). This indicates that, even though the casein degradation rates might not suffer from acidification, there was a slightly negative effect by acidification on the degradation efficiencies of casein measured as protein.

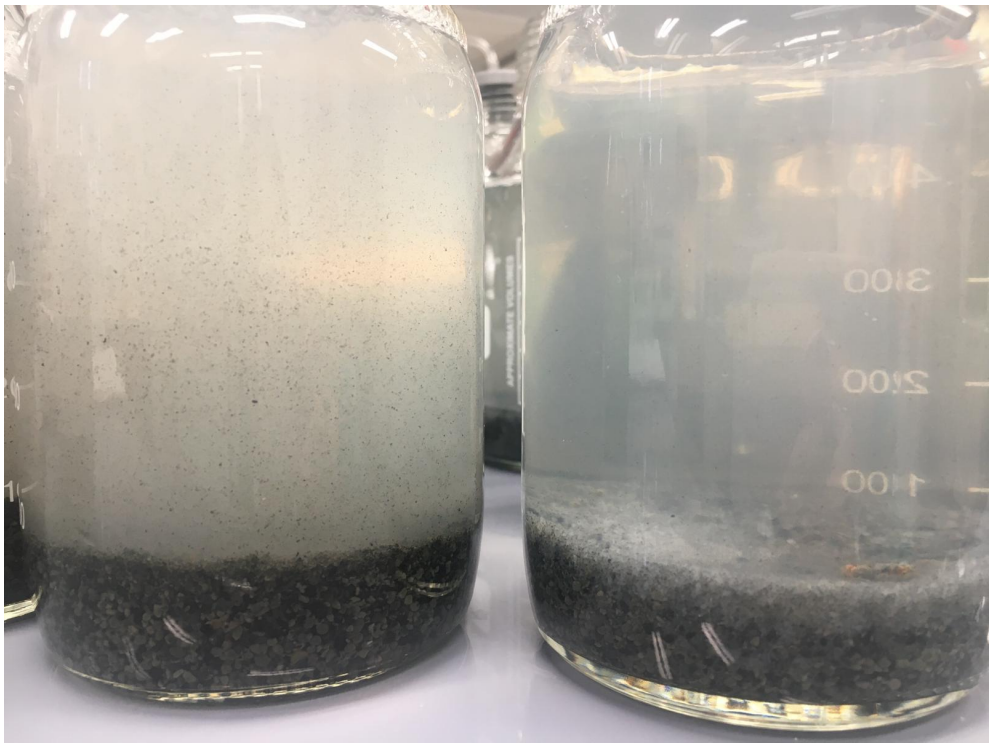

Figure 5.9: BMP bottles of both casein and lactose (left) and casein with VFAs (right). In both bottles biomass is settled on the bottom. Casein is nearly fully dissolved on the left, whereas precipitation can be observed on the biomass on the right in the form of casein flocs. The reason for this is the slightly lowered pH. The pH profiles are shown in section B.3.

Furthermore, there was no difference in COD degradation efficiency observed, which led to the assumption that intermediate products are converted to biogas

properly and no accumulation of VFAs occurred. This claim is also supported by the VFA profile depicted in Figure 5.7b.

Discussion for casein

The objective for the batch trials executed with casein was to determine the effect of lactose on the protein degradation based on various aspects. In a follow-up step, biological acidification was simulated by adding VFAs as substrate together with the protein. This was done to assess the applicability of such a pre-treatment to protein-rich substrate.

Overall, there was no significant positive or negative effect of lactose addition to casein observed during anaerobic digestion. However, a positive effect was documented during BMP trials where the BMP was significantly higher for the casein and lactose mixture than for pure lactose. An additional trial for pure casein is recommended to obtain values with less deviation in order to compare it to the casein and lactose trial. The success of co-digestion of protein-rich substrates together with more easily degradable substrate has already been reported by another research group (Hagos et al. [2017]). A study done by Brown et al. [2016] tested different ratios of casein whey and cow manure as digestion aid and reported a 78% increase in biogas production of primary sludge compared to the singular digestion of sludge. The increase thereof was attributed to the casein whey.

Furthermore, it has to be mentioned that process instabilities were caused due to the addition of a propionate:acetate ratio of 3:1, which was discussed with Biothane. However, the wastewater Biothane investigated was dairy industry effluent with a high percentage of whey proteins, which are soluble and inherently different from casein.

On the one hand, it was already determined by literature that lactose degrades via various pathways to an array of different VFAs (Hassan and Nelson [2012]). On the other hand, casein disassembles into amino acids, which only have two options: coupled (Stickland reaction) or uncoupled fermentation. Uncoupled fermentation is considered thermodynamically unfavourable, which makes Stickland reaction the more suitable fermentation pathway in nearly every case. Looking into the amino acids sequence of casein, it becomes apparent that acetic acid and not propionic acid is the dominant VFA produced (Ramsay and Pullammanappallil [2001]). This means that instabilities might not be as impactful such as reported in Figure 5.7a and 5.8a. The other inhibiting compound that might have an impact is butyric acid, which also requires specific conditions for proper degradation (van Lier et al. [2008]). To verify this, though, another acidification trial is recommended.

5.5 AMINO ACID ANALYSIS

This section provides a stoichiometric estimation of the VFA production from proteins that was already shortly discussed in the results section about the acidification of BSA and casein. However, since amino acids measurements for this project were not reliable there was no direct verification possible. Additionally, the chosen methodology is valid for a constant concentration of protein, which could not be provided by executing batch tests. Therefore, only an overall ratio was calculated and an attempt was made to compare with the obtained VFA production results.

Besides, an attempt was made to define the biological ammonia potential and comparing it to the theoretical ammonia potential.

For both proteins an overall reaction equation was set up:

$$CN_aH_bO_c + \alpha_{water}H_2O \rightarrow \alpha_{acet}CH_3COOH + \alpha_{prop}CH_3CH_2COOH + \alpha_{buty}CH_3CH_2CH_2COOH + \alpha_{vale}CH_3CH_2CH_2CH_2COOH + R$$

where the formula for casein was calculated as $CN_{0.3}H_{1.9}O_{0.5}$ and for BSA as $CN_{0.3}H_2O_{0.5}$. The R in the formula stands for other products such as CO_2, H_2, ATP and aromatic acids, which are generally necessary to keep a closed carbon balance, but are neglected for the ratio of VFAs produced. Additionally, ammonia is not included as it is analysed separately in a subsequent section.

5.5.1 VFA production from proteins

The analysis of both the amino acid sequence as well as the stoichiometric coefficients for VFAs are shown in Table 5.17 for casein and Table 5.18 for BSA, respectively. The exact calculations can be found in Appendix A.2.

The methodology suggested by Ramsay and Pullammanappallil [2001] breaks the protein down into its constituents and follows the Stickland fermentation until the VFA production. Some values stated in Table 5.17 and 5.18 showed a significant difference in theoretical and calculated values. The main reason for this discrepancy comes from the fact that the suggested methodology is applied to a continuous reactor where a stable influent concentration of casein at $6g \cdot L^{-1}$ is maintained. Instead, in this research project batch tests were set up, which means a direct translation to an up-scaled system is not possible.

Table 5.17: Stoichiometric coefficients for VFAs and ammonia from casein.

	Acetic acid	**Propionic acid**	**Butyric acid**	**Valeric acid**
mole /C-mole casein	0.108	0.016	0.041	0.038
% VFA from amino acids	53%	8%	20%	19%
% VFA from measurements	40 ± 1 %	15 ± 2%	22 ± 1%	20 ± 3%

Table 5.18: Stoichiometric coefficients for VFAs and ammonia from BSA.

	Acetic acid	**Propionic acid**	**Butyric acid**	**Valeric acid**
mole /C-mole BSA	0.129	0.010	0.051	0.034
% VFA from amino acids	58%	4%	23%	15%
% VFA from measurements	44 ± 2 %	16 ± 1%	16 ± 0%	24 ± 1%

By comparing the two proteins it seems that propionic acid was underestimated by the theoretical calculation in both cases. This might occur due to accumulation and thus retarded degradation. An opposite process was seen for acetic acid, which was overestimated by the theoretical approach, probably due to its fast degradation. Another reason for the deviation in results could be the occurrence of uncoupled amino acid fermentation, which is not a dominant reaction but might still take place to a lower extent. However, overall a difference of maximum 14% between theoretical and calculated values was observed.

5.5.2 Ammonia production from proteins

To define a theoretical ammonia potential the total amount of nitrogen in one gram of protein was determined by analysing the amino acid sequences of BSA and casein. The theoretical values as well as produced ammonia for BSA and casein is shown in Table 5.19.

What has already been stated is that the conversion efficiency of BSA and glucose (to be found in section 5.3) was significantly lower than the rest of the feeds. A similar trend was observed here with BSA and glucose showing the lowest ammonia released per gram of BSA in the substrate. A significantly lower value was also shown when 50% VFAs are added to the substrate. No change was observed for the 25% acidified substrate for BSA, which suggests a 25% acidification of the feed is beneficial to reach the potential of pure protein conversion.

Next, a similar scenario was depicted for casein. Values for pure BSA and casein showed no significant difference, meaning that both proteins provided in their soluble form were efficiently degraded and converted. Additionally, no significant difference was observed for the cases of lactose or VFA addition of 50% or 25%. This indicates that any degree of acidification applied could not reach the potential of pure casein to ammonia conversion. However, it was difficult to conclude for casein since conversion efficiency results were not reliable.

To summarise, it can be said that even though the potential of pure protein conversion could not be reached by the trials with added carbon sources the obtained values were still rather high and show good potential. For BSA, specifically, 25% acidification reached the observed values of pure protein, which deems the pretreatment up to this extent beneficial for anaerobic digestion.

Table 5.19: The theoretical ammonia potential is 0.17 and 0.16 $gN \cdot gProtein^{-1}$ for BSA and casein, respectively. Produced ammonia values were measured after t = 72h for BSA and t = 133h for casein. Values in the right column were calculated using equation 4.14.

	Produced ammonia (mgNH3-N/L)	$gN \cdot gProtein^{-1}$ released	% of theoretical value
BSA	284 ± 3	0.15	90 ± 1%
BSA + Glucose	238 ± 3	0.13	76 ± 1%
BSA (50% acidification)	261 ± 13	0.14	83 ± 4%
BSA (25% acidification)	270 ± 9	0.15	87 ± 3%
Casein	294 ± 4	0.14	88 ± 1%
Casein + Lactose	275 ± 0	0.13	82 ± 0%
Casein (50% acidification)	267 ± 7	0.13	80 ± 2%
Casein (25% acidification)	264 ± 9	0.13	79 ± 3%

6 GENERAL DISCUSSION

The objectives of this thesis were to gain understanding of the co-digestion of sugar and protein under anaerobic, mesophilic conditions, to test biological acidification as pre-treatment for a protein + sugar mixture, and to determine a biological ammonia potential for future applications. This was attempted by a literature study and lab experiments. Including all information gathered throughout this project, questions raised in chapter 3 are discussed in this chapter.

1. What is the impact of sugar on the rate and efficiency of the anaerobic degradation of proteins?

   First and foremost, there was no negative impact observed during the mixed trials of protein and sugar for all three proteins tested. A positive impact on the methane yield and process stability was observed in all cases, which was as expected based on similar observations reported in literature.

   Additionally, for both gelatin and BSA a significant increase in both protein degradation and methane production rates was observed after the addition of glucose. As already mentioned, this increase might have to do with the glucose substrate concentration. An inhibitory effect was assumed at a ratio of glucose to gelatin at 2:1 (Breure et al. [1986]). In this study, a ratio of 1:1 was applied, which led to no observable inhibition. Furthermore, an initial negative impact on the degradation rate was reported of a mixture of starch and glucose on BSA (Tommaso et al. [2003]). This could also have to do with the carbohydrates:BSA ratio as well as the addition of starch, which is a more complex carbohydrate than glucose.

   Lastly, no significant positive or negative effect of lactose addition to casein was observed. The addition of glucose was not investigated, which could produce different results. Lactose was chosen as a more common sugar of the dairy industry and was therefore investigated together with casein.

   Only one research group (Breure et al. [1986]) ever reported on the decreased degradation of protein (gelatin) by the addition of glucose, which they concluded from literature study. This could be attributed to the reduced production of proteases, the enzymes responsible for the cleavage of hydrogen bonds in between peptides. This would mean hydrolytic bacteria are inhibited by the addition of glucose, which has not been reported elsewhere. In principle, the hydrolytic fraction in biomass is inhibited only by elevated levels of VFAs, long-chain fatty acids (LCFAs), hydrogen partial pressure and humic acids (Amha et al. [2018]).

   Furthermore, it is reported that if propionic acid makes up 50% of the feed concentration both hydrolysis and methanogenesis of cellulose and glucose are inhibited (Siegert and Banks [2005]). Yet, in this research project only methanogenic and acidogenic inhibition was observed during the trials with increased propionate concentrations.

   Nothing similar has been reported for proteins, though. In fact, a relationship between protease activity and carbohydrates concentration has not been directly measured by any research group. That means that the effect on the hydrolytic biomass due to the co-existence of carbon sources remains unknown.

Within this research project, a co-utilisation of carbon sources is suggested. However, it is not a matter of protein vs. sugar but rather of amino acids vs. sugar. Considering that monomeric sugars are already hydrolised products of more complex carbohydrates, and thus easily available, the same should apply to the other carbon source in question. A very recent study published in 2019 (Wang et al. [2019]) compares different growth strategies of microbes on mixed carbon sources. Two strategies are discussed: diauxie (utilisation in sequence) and co-utilisation. It is stated that in general carbon sources entering a metabolic network at different locations are compatible for co-utilisation. A distinction is made between group A, which entails carbon sources entering the upper part of glycolysis, such as lactose and glucose, and group B, which entails sources joining at other points of the metabolic network, such as amino acids.

In short, the reason for diauxie is the preferred utilisation of one carbon source over the other by expressing the enzyme for only one of the two carbon sources. The reason for co-utilisation, however, would be the more economical usage of the carbon sources, based on their efficiency. This relates to a metabolic network where intermediate products can be produced from each carbon source. If microbial growth relies on the supply of more than one intermediate product, it is more beneficial for the organism to express enzymes for both carbon sources for energy-saving purposes.

This could differ for the two carbon sources based on where in the metabolic network they are found, and how many intermediary steps are needed for their utilisation. Based on the fact that the sugars, glucose and lactose, can still be traced during COD measurements throughout the experiments consecutive utilisation of substrates is less likely. Additionally, microorganisms such as *Tetrasphaera* are known to co-utilise amino acids and glucose (Liu et al. [2019a]). However, a microbial community analysis is needed to verify this.

2. What is the impact of pre-acidification on the rate and efficiency of the anaerobic degradation of proteins?

It was shown for both BSA and casein that the addition of VFAs can result in process instabilities in terms of methane production and degradation of VFAs. However, in terms of protein degradation rates, different behaviours are observed for casein and BSA. In the case of casein, the addition of VFAs does, on the one hand, not impact the protein degradation rates at all, even at 50% acidification. On the other hand, the highest protein degradation rate of BSA is observed at 25% acidification whereas the rate at the highest degree of VFAs (50%) shows an insignificant difference as compared to the pure BSA case. Concrete conclusions for casein are not possible, as the fitting of kinetics is rather poor.

By keeping the pH stable and above 7 through the addition of a buffer, major fluctuations during operation were prevented. Often, the combination of accumulation of VFAs and the resulting decrease in pH imposes an inhibition on the system (Amha et al. [2018]). Hence, also considering the severe process instabilities caused by 50% VFA as substrate, a lower degree of acidification is recommended.

It turns out the most crucial aspect of biological acidification is the ratio of VFAs produced. An analysis of the VFA composition of the feed shows that for each protein an indication of process instabilities can already be predicted if amino acid sequences are taken into account. Especially for protein-rich wastewater this can be a first step prior to application of a pre-treatment. Carbohydrates, however, degrade to VFAs via a variety of pathways, which can be steered by microbial selection or an adjustment in operational parameters.

3. How can the biological ammonia potential (BAP) of proteins be defined?

   The nitrogen content of proteins differs vastly and using a general conversion factor of 6.25 can result in over- or underestimations (Mariotti et al. [2008]). Amino acid sequences of almost any protein are freely available in online protein databases and are a direct way to determine the nitrogen content. The theoretical maximum is achieved if the whole protein is degraded and all ammonia is released. Ammonia production and consumption by the biomass, or addition thereof as nutrients, has to be deducted from the measured value to ensure only the produced ammonia is included. Mixtures of proteins can be considered as well by averaging ammonia produced per amino acid present in the structure.

   A precise definition of the BAP was not achieved, however, parameters to determine the successful conversion of proteins to ammonia were defined. The combination of the produced ammonia as stated in Table 5.19, and the conversion efficiencies, together with the degradation efficiency can be used to improve the anaerobic digestion process of protein-rich feed.

Next to the defined research questions, an amino acid analysis gave insight on the preferred fermentation pathways of amino acid-degrading bacteria. Based on the overlap of measured and theoretical values, it was assumed that the Stickland reaction was indeed the pre-dominant fermentation pathway. Deviations of the measurements could therefore be due to single amino-acid fermentation or measurement errors.

7 CONCLUSIONS AND RECOMMENDATIONS

7.1 CONCLUSIONS

The discussions and answers (Chapter 6) to the subquestions raised in Chapter 3 lead to the overall research question: *Can the degradability of proteins be improved through the co-digestion with easily degradable carbon sources?*

The degradability of proteins is **not** improved through the co-digestion of easily degradable carbon sources, but co-digestion and biological acidification make it possible to degrade a protein + sugar mixture without losing efficiency of the process. An improvement for casein is very likely, however, results are not strong enough to give an overall conclusion.

In summary it can be said, therefore, that co-digestion and pre-acidification are potential ways of improving the anaerobic digestion process of proteins. However, further research is needed to gain more understanding and a list of points to address is given in Section 7.2.

In short, the conclusions are:

- Co-digestion of proteins and sugars results in an improvement of both degradation rate and efficiency.
- The efficiency of biological acidification depends on the ratio of VFAs that results from the anaerobic digestion of proteins.
- Amino acid analysis is a valuable tool to understand and predict the production of VFAs from the anaerobic digestion of protein.
- The biological ammonia potential shows a high correlation with the conversion and degradation efficiency of proteins. Hence, it is a good indication of the completion of anaerobic digestion.

7.2 RECOMMENDATIONS

Some aspects of the co-digestion of proteins and sugars were addressed within this research project. However, further research is required to understand the bigger picture of this process. Here, several recommendations for further experiments are given.

1. During the executed batch tests ammonia concentrations were relatively low. In an up-scaled reactor where a constant loading rate can be applied the production of ammonia needs to be observed carefully. No inhibition was observed even at high free ammonia concentrations, except in combination with propionic acid, which was deemed more impactful. However, if pre-acidification is applied on protein-rich wastewater and propionic acid is produced in excess process stability cannot be guaranteed and biogas production might decrease. Therefore, based on how much ammonia can potentially be produced, there might be a trade-off to produce more ammonia and risking a decrease in biogas production, or vice versa. Thus, it is recommended to further assess the impact of high ammonia concentrations on the anaerobic digestion process to ensure that no major complications will occur.

2. The investigated compounds included proteins and sugars. However, it is necessary that lipids be investigated as well in order to represent the composition of wastewater more realistically. Especially slaughterhouse wastewater, of which for example BSA is a major compound, shows a high content of fats and sugars alike. It is generally known that lipids are troublesome compounds, which would make the anaerobic digestion of proteins even more difficult.

3. Last but not least, no experiments were conducted on microbiology. In order to analyse the reaction of enzyme production to co-digestion more experiments are needed to identify this. Adamczyk et al. [2003] used isotope labels to identify which organisms in a microbial community would consume a certain type of substrate. In a similar way, the consumption of protein with a certain label, such as ^{14}N, could be compared to the carbon of a sugar, such as ^{14}C. In that way, the behaviour of microorganisms that are exposed to the two carbon sources would be made clearer.

BIBLIOGRAPHY

Adamczyk, J., Hesselsoe, M., Iversen, N., Horn, M., Lehner, A., Nielsen, P. H., Schloter, M., Roslev, P., and Wagner, M. (2003). The Isotope Array, a New Tool That Employs Substrate-Mediated Labeling of rRNA for Determination of Microbial Community Structure and Function. *Applied and Environmental Microbiology*, 69(11):6875–6887.

Ahn, Y. H., Min, K. S., and Speece, R. E. (2001). Full scale uasb reactor performance in the brewery industry. *Environmental Technology (United Kingdom)*, 22(4):463–476.

Alexiou, I. E. (1998). *A Study of Pre-Acidification Reactor Design for Anaerobic Treatment of High Strength Industrial Wastewaters*. PhD thesis, University of Newcastle Upon Tyne.

Alexiou, I. E., Anderson, G. K., and Evison, L. M. (1994). Design of pre-acidificaiton reactos for the anaerobic treatment of industrial wastewaters. *Water Science and Technology*, 29(9):199–204.

Amha, Y. M., Anwar, M. Z., Brower, A., Jacobsen, C. S., Stadler, L. B., Webster, T. M., and Smith, A. L. (2018). Inhibition of anaerobic digestion processes : Applications of molecular tools. *Bioresource Technology*, 247:999–1014.

Ay, S., Weichgrebe, D., and Rosenwinkel, K. H. (2011). Determination of the hydrolysis constant using Anaerobic Batch Tests. *IWA Congress Anaerobic Digestion*, page 4.

Bader, J., Rauschenbach, P., and Simon, H. (1982). On a hitherto unknown fermentation path of several amino acids by proteolytic clostridia. *FEBS Letters*, 140(1):67–72.

Barker, H. (1981). Amino Acid Degradation. *Annual Reviews of Biochemistry*, 50:23–40.

Baskaran, K., Palmowski, L. M., and Watson, B. M. (2003). Wastewater reuse and treatment options for the dairy industry. *Water Science and Technology: Water Supply*, 3(3):85–91.

Berg, J. M., Tymoczko, J. L., and Stryer, L. (2006). *Biochemistry*. W. H. Freeman & Company.

Bharathiraja, B., Sudharsana, T., Jayamuthunagai, J., Praveenkumar, R., Chozhavendhan, S., and Iyyappan, J. (2018). Biogas production – A review on composition, fuel properties, feed stock and principles of anaerobic digestion. *Renewable and Sustainable Energy Reviews*, 90:570–582.

Bhat, M. Y., Dar, T. A., and Singh, L. R. (2016). Casein Proteins: Structural and Functional Aspects. *Intech*, page 13.

Bonk, F., Popp, D., Weinrich, S., Sträuber, H., and Kleinsteuber, S. (2018). Ammonia Inhibition of Anaerobic Volatile Fatty Acid Degrading Microbial Communities. *Frontiers in Microbiology*, 9:1–13.

Breure, A. M., Mooijman, K. A., and van Andel, J. G. (1986). Protein degradation in anaerobic digestion: influence of volatile fatty acids and carbohydrates on hydrolysis and acidogenic fermentation of gelatin. *Applied Microbiology and Biotechnology*, 24(5):426–431.

Brigham, C. (2018). Biopolymers: Biodegradable Alternatives to Traditional Plastics. *Green Chemistry*, pages 753–770.

Brown, N., Güttler, J., and Shilton, A. (2016). Overcoming the challenges of full scale anaerobic co-digestion of casein whey. *Renewable Energy*, 96:425–432.

Bustillo-Lecompte, C. F. and Mehrvar, M. (2017). Slaughterhouse Wastewater: Treatment, Management and Resource Recovery. *School of Enviromental Sciences*.

Carter, J. and Sagers, R. (1972). Ferrous ion-dependent L-serine dehydratase from Clostridium acidiurici. *Journal of Bacteriology*, 109(2):757–763.

Chang, S. W., Ye, Y., Liang, H., Ngo, H. H., Guo, W., Wang, J., Nguyen, D. D., and Liu, Y. (2018). A critical review on ammonium recovery from wastewater for sustainable wastewater management. *Bioresource Technology*, 268:749–758.

Cohen, A., Breure, A. M., Schmedding, D. J., Zoetemeyer, R. J., and van Andel, J. G. (1985). Significance of partial pre-acidification of glucose for methanogenesis in an anaerobic digestion process. *Applied Microbiology and Biotechnology*, 21(6):404–408.

Consortium, T. U. (2019). UniProt: a worldwide hub of protein knowledge.

Creighton, T. E. (1993). *Proteins : structures and molecular properties* . W.H. Freeman.

Elbeshbishy, E. and Nakhla, G. (2012). Batch anaerobic co-digestion of proteins and carbohydrates. *Bioresource Technology*, 116:170–178.

Elsden, S. R., Hilton, M. G., and Waller, J. M. (1976). The end products of the metabolism of aromatic amino acids by clostridia. *Archives of Microbiology*, 107:283–288.

Fowler, D., Coyle, M., Skiba, U., Sutton, M. A., Cape, J. N., Reis, S., Sheppard, L. J., Jenkins, A., Grizzetti, B., Galloway, J. N., Vitousek, P., Leach, A., Bouwman, A. F., Butterbach-Bahl, K., Dentener, F., Stevenson, D., Amann, M., and Voss, M. (2013). The global nitrogen cycle in the Twentyfirst century. *Philosophical Transactions of the Royal Society B: Biological Sciences*, 368(1621):1–13.

Galloway, J. N. (1998). The global nitrogen cycle: changes and consequences. *Environmental Pollution*, 102(1):15–24.

Gavala, H. N., Angelidaki, I., and Ahring, B. K. (2003). Kinetics and Modeling of Anaerobic Digestion Process. *Advances in Biochemical Engineering/ Biotechnology*, 81:57–93.

GMIA (2019). GMIA, Gelatin Handbook. Technical report, Gelatin Manufacturers Institute Of America.

Göblös, S., Portörő, P., Bordás, D., Kálmán, M., and Kiss, I. (2008). Comparison of the effectivities of two-phase and single-phase anaerobic sequencing batch reactors during dairy wastewater treatment. *Renewable Energy*, 33(5):960–965.

Hafner, S. (2019). Calculation of biochemical methane potential (BMP).

Hagos, K., Zong, J., Li, D., Liu, C., and Lu, X. (2017). Anaerobic co-digestion process for biogas production: Progress, challenges and perspectives. *Renewable and Sustainable Energy Reviews*, 76:1485–1496.

Hardman, J. and Stadtman, T. (1960). Metabolism of omega-amino acids. I. Fermentation of gamma-aminobutyric acid by Clostridium aminobutyricum n. sp. *Journal of Bacteriology*, 79:544–548.

Hassan, A. and Nelson, B. (2012). Invited review: Anaerobic fermentation of dairy food wastewater. *Journal of Dairy Science*, 95(11):6188–6203.

Hejnfelt, A. and Angelidaki, I. (2009). Anaerobic digestion of slaughterhouse by-products. *Biomass and Bioenergy*, 33(8):1046–1054.

Holliger, C., Alves, M., Andrade, D., Angelidaki, I., Astals, S., Baier, U., Bougrier, C., Buffière, P., Carballa, M., de Wilde, V., Ebertseder, F., Fernández, B., Ficara, E., Fotidis, I., Frigon, J.-C., de Laclos, H. F., Ghasimi, D. S. M., Hack, G., Hartel, M., Heerenklage, J., Horvath, I. S., Jenicek, P., Koch, K., Krautwald, J., Lizasoain, J., Liu, J., Mosberger, L., Nistor, M., Oechsner, H., Oliveira, J. V., Paterson, M., Pauss, A., Pommier, S., Porqueddu, I., Raposo, F., Ribeiro, T., Rüsch Pfund, F., Strömberg, S., Torrijos, M., van Eekert, M., van Lier, J., Wedwitschka, H., and Wierinck, I. (2016). Towards a standardization of biomethane potential tests. *Water Science and Technology*, 74(11):2515–2522.

Hoogerbrugge, R., Geilenkirchen, G., den Hollander, H., van der Swaluw, E., Visser, S., de Vries, W., and Wichink Kruit, R. (2019). Grootschalige concentratie- en depositiekaarten Nederland.

Kalyuzhnyi, S., Batstone, D., Vavilin, V., Pavlostathis, S., Siegrist, H., Sanders, W., Rozzi, A., Angelidaki, I., and Keller, J. (2002). The IWA Anaerobic Digestion Model No 1 (ADM1). *Water Science and Technology*, 45(10):65–73.

Klein, H., Gauss, M., Nyiri, A., and Tsyro, S. (2019). Transboundary air pollution by main pollutants (S, N, O3) and PM in 2017. The Netherlands.

Lettinga, G. and Hulshoff Pol, L. W. (1991). UASB-process design for various types of wastewaters. *Water Science and Technology*, 24(8):87–107.

Li, N., Xue, Y., Chen, S., Takahashi, J., Dai, L., and Dai, X. (2017). Methanogenic population dynamics regulated by bacterial community responses to protein-rich organic wastes in a high solid anaerobic digester. *Chemical Engineering Journal*, 317:444–453.

Lin, C.-Y., Lay, C.-H., and Chen, C.-C. (2017). High-Strength Wastewater Treatment Using Anaerobic Processes. *Current Developments in Biotechnology and Bioengineering*, pages 321–357.

Lin, L. and Xu, F. (2019). Biological treatment of organic materials for energy and nutrients production—Anaerobic digestion and composting. *Advances in Bioenergy*, 4:121–181.

Lin, R., Cheng, J., and Murphy, J. D. (2018). Inhibition of thermochemical treatment on biological hydrogen and methane co-production from algae-derived glucose/glycine. *Energy Conversion and Management*, 158:201–209.

Liu, R., Hao, X., Chen, Q., and Li, J. (2019a). Research advances of Tetrasphaera in enhanced biological phosphorus removal : A review. *Water Research*, 166:1–10.

Liu, Y., Ngo, H. H., Guo, W., Peng, L., Wang, D., and Ni, B. (2019b). The roles of free ammonia (FA) in biological wastewater treatment processes: A review. *Environment International*, 123:10–19.

Lowry, O. H. and. Rosebrough, N., Randall, R., and Lewis, F. (1994). Protein Measurement with the Folin Phenol Reagent. *Analytical Biochemistry*, 217(2):220–230.

Mariotti, F., Tomé, D., and Mirand, P. P. (2008). Converting nitrogen into protein - Beyond 6.25 and Jones' factors. *Critical Reviews in Food Science and Nutrition*, 48(2):177–184.

Mead, G. (1971). The amino acid-fermenting clostridia. *Journal of General Microbiology*, 67(1):47–56.

Mehmood, A. M. M. T., Iyer, A. B., Arif, S., Junaid, M., Khan, R. S., Nazir, W., and Khalid, N. (2019). Whey Protein-Based Functional Energy Drinks Formulation and Characterization. *Sports and Energy Drinks*, 10:161–181.

Meister, A., Sober, H., and Tice, S. (1951). Enzymatic decarboxylation of aspartic acid to alpha-alanine. *Journal of Biological Chemistry*, 189(2):577–590.

Nanninga, H. J. and Gottschal, J. C. (1985). Amino acid fermentation and hydrogen transfer in mixed cultures. *FEMS Microbiology Ecology*, 31:261–269.

Omil, F., Méndez, R., and Lema, J. M. (1995). Anaerobic treatment of saline wastewaters under high sulphide and ammonia content. *Bioresource Technology*, 54(3):269–278.

Pavlostathis, S. and Giraldo-Gomez, E. (1991). Kinetics of anaerobic treatment: A critical review. *Critical Reviews in Environmental Control*, 21(5-6):411–490.

Perna, V., Castelló, E., Wenzel, J., Zampol, C., Lima, D. F., Borzacconi, L., Varesche, M., Zaiat, M., and Etchebehere, C. (2013). Hydrogen production in an upflow anaerobic packed bed reactor used to treat cheese whey. *International Journal of Hydrogen Energy*, 38(1):54 – 62. European Fuel Cell 2011.

Rajagopal, R., Massé, D. I., and Singh, G. (2013). A critical review on inhibition of anaerobic digestion process by excess ammonia. *Bioresource Technology*, 143:632–641.

Ramsay, I. and Pullammanappallil, P. (2001). Protein degradation during anaerobic wastewater treatment. *Biodegradation*, 12:247–257.

Seto, B. (1980). The Stickland Reaction. *Diversity in Bacterial Respiratory Systems*, 2:49–64.

Siegert, I. and Banks, C. (2005). The effect of volatile fatty acid additions on the anaerobic digestion of cellulose and glucose in batch reactors. *Process Biochemistry*, 40(11):3412–3418.

Siegrist, H., Vogt, D., Garcia-Heras, J. L., and Gujer, W. (2002). Mathematical model for meso- and thermophilic anaerobic sewage sludge digestion. *Environmental Science and Technology*, 36(5):1113–1123.

Sun, C., Xia, A., Fu, Q., Huang, Y., Lin, R., and Murphy, J. D. (2019). Effects of pretreatment and biological acidification on fermentative hydrogen and methane co-production. *Energy Conversion and Management*, 185:431–441.

Surendra, K., Takara, D., Hashimoto, A. G., and Khanal, S. K. (2014). Biogas as a sustainable energy source for developing countries: Opportunities and challenges. *Renewable and Sustainable Energy Reviews*, 31:846–859.

Tobias, J. W., Shrader, T. E., Rocap, G., and Varshavsky, A. (1991). The N-end rule in bacteria. *Science*, 254(5036):1374–1377.

Tommaso, G., Ribeiro, R., Varesche, M. B. A., Zaiat, M., and Foresti, E. (2003). Influence of multiple substrates on anaerobic protein degradation in a packed-bed bioreactor. *Water Science and Technology*, 48(6):23–31.

Townsend, A. R., Howarth, R. W., Bazzaz, F. A., Booth, M. S., Cleveland, C. C., Collinge, S. K., Dobson, A. P., Epstein, P. R., Holland, E. A., Keeney, D. R., Mallin, M. A., Rogers, C. A., Wayne, P., and Wolfe, A. H. (2003). Human Health Effects of a changing global nitrogen cycle. *Frontiers in Ecology and the Environment*, 1:240–246.

Traversi, D., Bonetta, S., Degan, R., Villa, S., Porfido, A., Bellero, M., Carraro, E., and Gilli, G. (2013). Environmental Advances Due to the Integration of Food Industries and Anaerobic Digestion for Biogas Production: Perspectives of the Italian Milk and Dairy Product Sector. *Bioenergy Research*, 6(3):851–863.

Uçkun Kiran, E., Stamatelatou, K., Antonopoulou, G., and Lyberatos, G. (2016). Production of biogas via anaerobic digestion. *Handbook of Biofuels Production*, 2:259–301.

Valera-Medina, A., Xiao, H., Owen-Jones, M., David, W., and Bowen, P. (2018). Ammonia for power. *Progress in Energy and Combustion Science*, 69:63–102.

van Lier, J. B., Mahmoud, N., and Zeeman, G. (2008). *Biological wastewater treatment: principles, modeling and design - Chapter 16: Anaerobic wastewater treatment*. IWA Publishing.

Varshavsky, A. (1996). The N-end rule: Functions, mysteries, uses. *Proceedings of the National Academy of Sciences of the United States of America*, 93:12142–12149.

Vavilin, V., Fernandez, B., Palatsi, J., and Flotats, X. (2008). Hydrolysis kinetics in anaerobic degradation of particulate organic material: An overview. *Waste Management*, 28(6):939–951.

Vidra, A. and Németh, Á. (2018). Bio-produced propionic acid: A review. *Periodica Polytechnica Chemical Engineering*, 62(1):57–67.

Vitousek, P., Aber, J., Howarth, R., Likens, G., Matson, P., Schindler, D., Schlesinger, W., and Tilman, D. (1997). Human alteration of the global nitrogen cycle: Sources and consequences. *Ecological Applications*, 7(3):737–750.

Walsh, G. (2014). *Proteins : Biochemistry and Biotechnology* . John Wiley and Sons.

Wang, J. Y., Xu, H. L., and Tay, J. H. (2002). A hybrid two-phase system for anaerobic digestion of food waste. *Water Science and Technology*, 45(12):159–165.

Wang, X., Xia, K., Yang, X., and Tang, C. (2019). Growth strategy of microbes on mixed carbon sources. *Nature Communications*, 10(1):1–7.

Wang, Y. (2018). Energy Efficiency and Emissions Analysis of Ammonia, Hydrogen, and Hydrocarbon Fuels. *Journal of Energy and Natural Resources*, 7(1):47.

Wirth, R., Bagi, Z., Maróti, G., Kovács, K. L., Kovács, E., and Rákhely, G. (2013). Biogas Production from Protein-Rich Biomass: Fed-Batch Anaerobic Fermentation of Casein and of Pig Blood and Associated Changes in Microbial Community Composition. *PLoS ONE*, 8(10):1–18.

Yu, H. Q. and Fang, H. H. (2003). Acidogenesis of gelatin-rich wastewater in an upflow anaerobic reactor: Influence of pH and temperature. *Water Research*, 37(1):55–66.

A APPENDIX A: METHODOLOGY

A.1 AMINO ACID SEQUENCES

Ratio of amino acids of gelatin retrieved from GMIA [2019]:

Table A.1: Percentages of amino acids of gelatin)

Amino acid	%
Asp	16.65
Glu	0.71
Ser	1.86
Gly	23.05
His	0.59
Thr	2.98
Ala	10.16
Pro	13.57
Arg	9.2
Tyr	1.13
Val	1.76
Met	2.3
Cys	0.13
Ile	0.13
Leu	2.74
Phe	2.73
Lys	4.25
Hyp	6.01

Amino acid sequence BSA retrieved from Consortium [2019]:
DTHKSEIAHRFKDLGEEHFKGLVLIAFSQYLQQCPFDEHVKLVNELTEFAKTCVADESHAGCE
KSLHTLFGDELCKVASLRETYGDMADCCEKQEPERNECFLSHKDDSPDLPKLKPDPNTLCDE
FKADEKKFWGKYLYEIARRHPYFYAPELLYYANKYNGVFQECCQAEDKGACLLPKIETMREK
VLTSSARQRLRCASIQKFGERALKAWSVARLSQKFPKAEFVEVTKLVTDLTKVHKECCHGDLL
ECADDRADLAKYICDNQDTISSKLKECCDKPLLEKSHCIAEVEKDAIPENLPPLTADFAEDKD
VCKNYQEAKDAFLGSFLYEYSRRHPEYAVSVLLRLAKEYEATLEECCAKDDPHACYSTVFDKL
KHLVDEPQNLIKQNCDQFEKLGEYGFQNALIVRYTRKVPQVSTPTLVEVSRSLGKVGTRCCTK
PESERMPCTEDYLSLILNRLCVLHEKTPVSEKVTKCCTESLVNRRPCFSALTPDETYVPKAFDE
KLFTFHADICTLPDTEKQIKKQTALVELLKHKPKATEEQLKTVMENFVAFVDKCCAA

Amino acid sequence casein retrieved from Consortium [2019]:
RPKHPIKHQGLPQEVLNENLLRFFVAPFPEVFGKEKVNELSKDIGSESTEDQAMEDIKQM
EAESISSSEEIVPNSVEQKHIQKEDVPSERYLGYLEQLLRLKKYKVPQLEIVPNSAEERLHS
MKEGIHAQQKEPMIGVNQELAYFYPELFRQFYQLDAYPSGAWYYVPLGTQYTDAPSFSDIPNP
IGSENSEKTTMPLW

A.2 STOICHIOMETRY OF PROTEIN DEGRADATION

In a first attempt, the Stickland reactions of each amino acid were summarised in Table A.2.

Next, the overall stoichiometry from protein to VFAs was determined as shown in Table A.3 for BSA and A.5 for casein, respectively. The coefficients were then multiplied by the amino acid contents, which are based on one carbon mole of protein, and summed to give an overall stoichiometric coefficient.

In the following step, each amino acid is normalised per C-mole protein and stoichiometric coefficients are calculated for each VFA produced per mole of C-mole BSA (Table A.4) and casein (Table A.6).

In a last step, the stoichiometric coefficients are put into context with the VFA measurements obtained from batch experiments.

Table A.2: Stoichiometry for amino acid fermentation (catabolic reactions only)

No.	Reaction	Reference
1	$C_6H_{13}O_2N(\text{Leu}) + 2H_2O \rightarrow C_5H_{12}O_2(\text{3-methylbutyrate}) + NH_3 + CO_2 + 2H_2 + \text{ATP}$	Mead [1971]; Elsden et al. [1976]
2	$C_6H_{13}O_2N(\text{Ile}) + 2H_2O \rightarrow C_5H_{10}O_2(\text{2-methylbutyrate}) + NH_3 + CO_2 + 2H_2 + \text{ATP}$	Mead [1971]; Elsden et al. [1976]
3	$C_5H_{11}O_2N(\text{Val}) + 2H_2O \rightarrow C_4H_8O_2(\text{2-methylpropionate}) + NH_3 + CO_2 + 2H_2 + \text{ATP}$	Mead [1971]; Elsden et al. [1976]
4	$C_9H_{11}O_2N(\text{Phe}) + 2H_2O \rightarrow C_8H_8O_2(\text{phenylacetate}) + NH_3 + CO_2 + 2H_2 + \text{ATP}$	Elsden et al. [1976]
5	$C_9H_{11}O_3N(\text{Tyr}) + 2H_2O \rightarrow C_8H_8O_3(\text{hydroxyphenyl acetate}) + NH_3 + CO_2 + 2H_2 + \text{ATP}$	Elsden et al. [1976]
6	$C_{11}H_{12}O_3N_2(\text{Trp}) + 2H_2O \rightarrow C_{10}H_9O_2N(\text{indole acetate}) + NH_3 + CO_2 + 2H_2 + \text{ATP}$	Elsden et al. [1976]
7	$C_2H_5O_2N(\text{Gly}) + H_2 \rightarrow C_2H_4O_2(\text{acetate}) + NH_3$	Seto [1980]
8	$C_3H_7O_2N(\text{Ala}) + 2H_2O \rightarrow C_2H_4O_2(\text{acetate}) + NH_3 + CO_2 + 2H_2 + \text{ATP}$	Bader et al. [1982]
9	$C_3H_6O_2NS(\text{Cys}) + 2H_2O \rightarrow C_2H_4O_2(\text{acetate}) + NH_3 + CO_2 + H_2S + 1/2H_2\text{ATP}$	Barker [1981]
10	$C_5H_{11}O_2NS(\text{Met}) + 2H_2O \rightarrow C_3H_6O_2(\text{propionate}) + NH_3 + CO_2 + CH_3SH + H_2 + \text{ATP}$	Ramsay and Pullammanappallil [2001]
11	$C_3H_7O_3N(\text{Ser}) + H_2O \rightarrow C_2H_4O_2(\text{acetate}) + NH_3 + CO_2 + H_2 + \text{ATP}$	Carter and Sagers [1972]
12	$C_4H_9O_3N(\text{Thr}) + H_2O \rightarrow C_2H_4O_2(\text{acetate}) + 1/2C_4H_8O_2(\text{butyrate}) + NH_3 + \text{ATP}$	Hardman and Stadtman [1960]
13	$C_4H_7O_4N(\text{Asp}) + 2H_2O \rightarrow C_2H_4O_2(\text{acetate}) + NH_3 + 2CO_2 + 2H_2 + 2\text{ATP}$	Meister et al. [1951]
14	$C_5H_9O_4N(\text{Glu}) + H_2O \rightarrow C_2H_4O_2(\text{acetate}) + 1/2C_4H_8O_2(\text{butyrate}) + NH_3 + CO_2 + 2\text{ATP}$	Hardman and Stadtman [1960]
15	$C_6H_9O_2N_3(\text{His}) + 4H_2O \rightarrow CH_3ON(\text{formamide}) + C_2H_4O_2(\text{acetate}) + 1/2C_4H_8O_2(\text{butyrate}) + 2NH_3 + CO_2 + 2\text{ATP}$	Barker [1981]
16	$C_6H_{14}O_2N_4(\text{Arg}) + 6H_2O \rightarrow C_2H_4O_2(\text{acetate}) + 4NH_3 + 2CO_2 + 3H_2 + 2\text{ATP}$	Barker [1981]
17	$C_5H_9O_2N(\text{Pro}) + H_2O + H_2 \rightarrow 1/2C_2H_4O_2(\text{acetate}) + 1/2C_3H_6O_2(\text{propionate}) + 1/2C_5H_{10}O_2(\text{valerate}) + NH_3$	Mead [1971]; Elsden et al. [1976]
18	$C_6H_{14}O_2N_2(\text{Lys}) + 2H_2O \rightarrow C_2H_4O_2(\text{acetate}) + C_4H_8O_2(\text{butyrate}) + 2NH_3 + \text{ATP}$	Elsden et al. [1976]; Barker [1981]

Amino acid composition of BSA											
							multiplied				
	moles	**C**	**N**	**H**	**O**	**S**	**C**	**N**	**H**	**O**	**S**
Asp	40	4	2	8	3		4	4	16	6	0
Glu	59	5	1	9	4		5	1	9	4	0
Ser	28	3	1	7	3		3	1	7	3	0
Gly	16	2	1	5	2		2	1	5	2	0
His	17	6	3	9	2		18	9	27	6	0
Thr	34	4	1	9	3		4	1	9	3	0
Ala	46	3	1	7	2		3	1	7	2	0
Pro	28	5	1	9	2		5	1	9	2	0
Arg	23	6	4	14	2		24	16	56	8	0
Tyr	20	9	1	11	3		9	1	11	3	0
Val	36	5	1	11	2		5	1	11	2	0
Met	4	5	1	11	2	1	5	1	11	2	1
Cys	35	3	1	7	2	1	3	1	7	2	1
Ile	14	6	1	13	2		6	1	13	2	0
Leu	61	6	1	13	2		6	1	13	2	0
Phe	27	9	1	11	2		9	1	11	2	0
Lys	59	6	2	14	2		12	4	28	4	0
Asn	14	4	1	7	4		4	1	7	4	0
Trp	2	11	2	12	2		22	4	24	4	0
Gln	20	5	2	10	3		10	4	20	6	0
Sum		**107**	**29**	**197**	**49**	**2**	**159**	**55**	**301**	**69**	**2**
							Formula for BSA for C = 1				
							1,0	0,3	2,0	0,5	0,0

Table A.3: Number of amino acids in one BSA protein. The formula for BSA was calculated according to an elemental composition analysis.

Amino acid composition of BSA	mole AA / C-mole protein	Acetic acid (mole/mole AA)		Propionic acid (mole/mole AA)		Butyric acid (mole/mole AA)		Valeric acid (mole/mole AA)		Ammonia (mole NH_3/mole AA)	
Asp	0,0136	1	0,0136		0		0		0	1	0,0136
Glu	0,0201	1	0,0201		0	0,5	0,0101		0	1	0,0201
Ser	0,0095	1	0,0095		0		0		0	1	0,0095
Gly	0,0055	1	0,0054		0		0		0	1	0,0055
His	0,0058	1	0,0058		0	0,5	0,0029		0	2	0,0116
Thr	0,0116	1	0,0116		0	0,5	0,0058		0	1	0,0116
Ala	0,0157	1	0,0157		0		0		0	1	0,0156
Pro	0,0095	0,5	0,0048	0,5	0,0048		0	0,5	0,0048	1	0,0095
Arg	0,0078	0,5	0,0039	0,5	0,0039		0	0,5	0,0039	4	0,0313
Tyr	0,0068	1	0,0068		0		0		0	1	0,0068
Val	0,0123		0		0	1	0,0123		0	1	0,0123
Met	0,0014		0	1	0,0014		0		0	1	0,0014
Cys	0,0119	1	0,0119		0		0		0	1	0,0119
Ile	0,0048		0		0		0	1	0,0048	1	0,0048
Leu	0,0208		0		0		0	1	0,0208	1	0,0208
Phe	0,0092		0		0		0		0	1	0,0092
Lys	0,0201	1	0,0201		0	1	0,0201		0	2	0,0402
Asn	0,0048		0		0		0		0	1	0,0048
Trp	0,0007		0		0		0		0	1	0,0007
Gln	0,0068		0		0		0		0	1	0,007
Sum	**0,1986**	**0,129**		**0,010**		**0,051**		**0,034**		**0,248**	

Table A.4: Calculation of stoichiometric coefficients for four volatile fatty acids from BSA.

Amino acid composition of casein											
							multiplied				
	moles	**C**	**N**	**H**	**O**	**S**	**C**	**N**	**H**	**O**	**S**
Asp	7	4	2	8	3		28	14	56	21	0
Glu	25	5	1	9	4		125	25	225	100	0
Ser	16	3	1	7	3		48	16	112	48	0
Gly	9	2	1	5	2		18	9	45	18	0
His	5	6	3	9	2		30	15	45	10	0
Thr	5	4	1	9	3		20	5	45	15	0
Ala	9	3	1	7	2		27	9	63	18	0
Pro	17	5	1	9	2		85	17	153	34	0
Arg	6	6	4	14	2		36	24	84	12	0
Tyr	10	9	1	11	3		90	10	110	30	0
Val	11	5	1	11	2		55	11	121	22	0
Met	5	5	1	11	2	1	25	5	55	10	5
Cys	0	3	1	7	2	1	0	0	0	0	0
Ile	11	6	1	13	2		66	11	143	22	0
Leu	17	6	1	13	2		102	17	221	34	0
Phe	8	9	1	11	2		72	8	88	16	0
Lys	14	6	2	14	2		84	28	196	28	0
Asn	8	4	1	7	4		32	8	56	32	0
Trp	2	11	2	12	2		22	4	24	4	0
Gln	14	5	2	10	3		70	28	140	42	0
Sum		**107**	**29**	**197**	**49**	**2**	**1035**	**264**	**1982**	**516**	**5**

Table A.5: Number of amino acids in one casein protein. The formula for casein was calculated according to an elemental composition analysis.

Amino acid composition of casein	mole AA / C-mole protein	Acetic acid (mole/mole AA)		Propionic acid (mole/mole AA)		Butyric acid (mole/mole AA)		Valeric acid (mole/mole AA)		Ammonia (mole NH_3/mole AA)	
Asp	0,0068	1	0,0068		0		0		0	1	0,0068
Glu	0,0242	1	0,0242		0	0,5	0,0121		0	1	0,0242
Ser	0,0155	1	0,0155		0		0		0	1	0,0155
Gly	0,0087	1	0,0087		0		0		0	1	0,0087
His	0,0048	1	0,0048		0	0,5	0,0024		0	2	0,0097
Thr	0,0048	1	0,0048		0	0,5	0,0024		0	1	0,0048
Ala	0,0087	1	0,0087		0		0		0	1	0,0087
Pro	0,0164	0,5	0,0082	0,5	0,0082		0	0,5	0,0082	1	0,0164
Arg	0,0058	0,5	0,0029	0,5	0,0029		0	0,5	0,0029	4	0,0232
Tyr	0,0097	1	0,0097		0		0		0	1	0,0097
Val	0,0106		0		0	1	0,0106		0	1	0,0106
Met	0,0048		0	1	0,0048		0		0	1	0,0048
Cys	0,0000	1	0		0		0		0	1	0
Ile	0,0106		0		0		0	1	0,0106	1	0,0106
Leu	0,0164		0		0		0	1	0,0164	1	0,0164
Phe	0,0077		0		0		0		0	1	0,0077
Lys	0,0135	1	0,0135		0	1	0,0135		0	2	0,0271
Asn	0,0077		0		0		0		0	1	0,0077
Trp	0,0019		0		0		0		0	1	0,0019
Gln	0,0135		0		0		0		0	1	0,0135
Sum	**0,1923**	**0,108**		**0,016**		**0,041**		**0,038**		**0,228**	

Table A.6: Calculation of stoichiometric coefficients for four volatile fatty acids from casein.

A.3 CODE FOR KINETIC MODELLING

```
# -*- coding: utf-8 -*-
"""
Created on Fri Feb 14 10:58:00 2020

@author: boden
"""


import matplotlib.pyplot as plt
import numpy as np
from scipy.optimize import curve_fit

bgvmax = max(data.BGV_avg) #define the highest methane volume
    for substrate BGV
bgv = data.BGV_avg[:210] #retrieve methane data from excel
    file
t = np.linspace(0,209,210) #time step
h = np.zeros(len(t)) #empty array to be filled with
    calculated values for production coefficient

#
def fun(t,k): #define function according to first-order rate
    kinetics
    for i in range(len(t)-1):
        h[i] = (bgvmax*(1-np.exp(-k*t[i])))
        h[i+1] = h[i]
    return h
#
popt, pcov = curve_fit(fun, t, bgv) #use the curve fitting
    function to find the best coefficient value
#
p = np.corrcoef(h,bgv) #correlation coefficient to determine
    the fit of data to model

plt.plot(fun(t,popt)) #plot the model data over time
plt.plot(t,bgv) #plot the real data over time
plt.xlabel('Time (hours)',  fontdict=font)
plt.ylabel('Cumulative Methane Production (NLCH4)')
plt.legend(['Model', 'Data'], loc='lower right', fontsize=14)
plt.tick_params(labelsize=12)
plt.grid(linestyle=':', linewidth = 0.5)
plt.tight_layout()
```

B APPENDIX B: RESULTS

B.1 BIOGAS COMPOSITION

The different gases representing the total biogas composition were analysed and are given in Table B.1.

Table B.1: Methane and carbon dioxide percentages in biogas of anaerobically digested proteins. Experiments were performed in duplicates with the deviation columns showing the difference from the average in percent.

	CO_2 [%]	**Deviation [%]**	**CH_4 [%]**	**Deviation [%]**
Gelatin	16.0	0.0	82.0	0.0
BSA	19.5	0.1	78.5	0.1
Casein	17.5	0.1	80.0	0.0

The methane values for these compounds were in range of what is reported in literature (Surendra et al. [2014]; Bharathiraja et al. [2018]). Gelatin showed the highest methane percentage with a fraction of 82% being produced as CH_4. Accordingly, it also showed the lowest concentration of carbon dioxide at 16%. BSA and casein showed a similar distribution with 78.5% and 80% of methane and 19.5% and 17.5 % of carbon dioxide, respectively.

B.2 KINETIC ANALYSIS

B.2.1 Batch 2: Gelatin and BSA

Table B.2: Kinetics for the first gelatin and BSA trials

	Gelatin	Glucose	BSA	BSA + Glucose
k_{CH4} (d^{-1})	0.48	1.36	0.44	1.01
R^2	0.99	0.99	0.97	0.99
$k_{Protein}$ (d^{-1})	1.49	-	0.81	1.09
R^2	0.92	-	0.93	0.97

B.2.2 Batch 3: Gelatin and casein

No kinetic rate of methane production could be calculated for the casein trial depicted in table B.3 due to a gas leakage in the set-up.

Table B.3: Kinetics for the first gelatin and casein trials

	Gelatin	Lactose	Casein	Casein + Lactose	Gelatin + Glucose
k_{CH4} (d^{-1})	0.37	1.35	-	0.68	0.57
R^2	0.99	0.96	-	0.96	0.98
$k_{Protein}$ (d^{-1})	0.78	-	0.98	0.84	1.56
R^2	0.91	-	0.75	0.69	0.99

B.2.3 Batch 4: BSA acidification trial

Only a BMP test was executed with gelatin depicted in table B.4, which is why no protein rates are available.

Table B.4: Kinetics for the BSA acidification trial

	Gelatin	BSA	BSA + Glucose	BSA + VFAs	BSA + Glucose + VFAs
k (d^{-1})	0.38	0.69	1.07	0.33	0.73
R^2	0.99	0.98	0.99	0.99	0.99
$k_{Protein}$ (d^{-1})	-	0.57	0.68	0.58	0.70
R^2	-	0.95	0.98	0.99	0.98

B.2.4 Batch 5: Casein acidification trial

Only a BMP test was executed with gelatin depicted in table B.5, which is why no protein rates are available.

Table B.5: Kinetics for the casein acidification trial

	Gelatin	Casein	Casein + Lactose	Casein + VFAs	Casein + Lactose + VFAs
k (d^{-1})	0.47	0.50	0.79	0.33	0.60
R^2	0.99	0.99	0.97	0.98	0.99
$k_{Protein}$ (d^{-1})	-	0.18	0.13	0.16	0.16
R^2	-	0.92	0.86	0.57	0.67

B.3 PH PROFILES

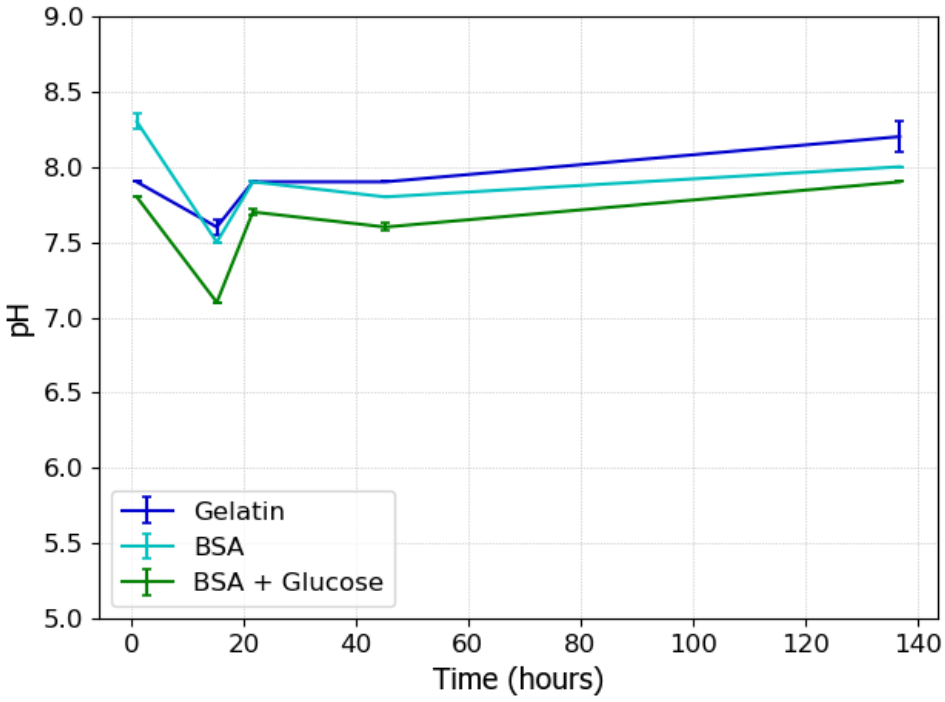

Figure B.1: pH data over a period of 133 hours for gelatin (dark blue), BSA (cyan) and BSA + glucose (green).

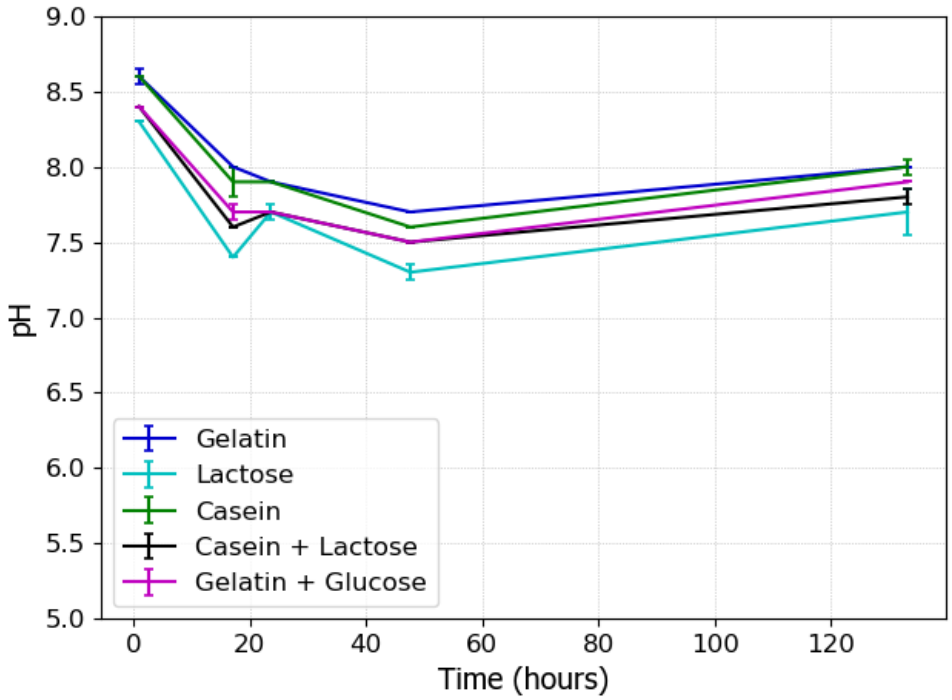

Figure B.2: pH data over a period of 130 hours for gelatin (dark blue), lactose (cyan), casein (green), casein + lactose (black) and gelatin + glucose (magenta).

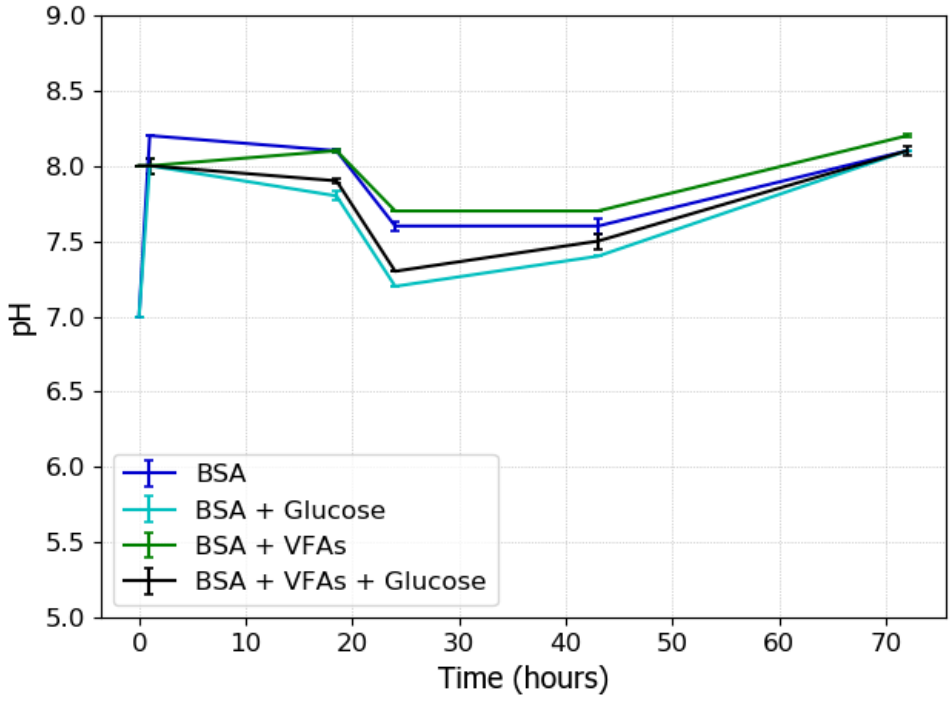

Figure B.3: pH data over a period of 72 hours for BSA (dark blue), BSA + glucose (cyan), BSA + VFAs (green) and BSA + VFAs + glucose (black).

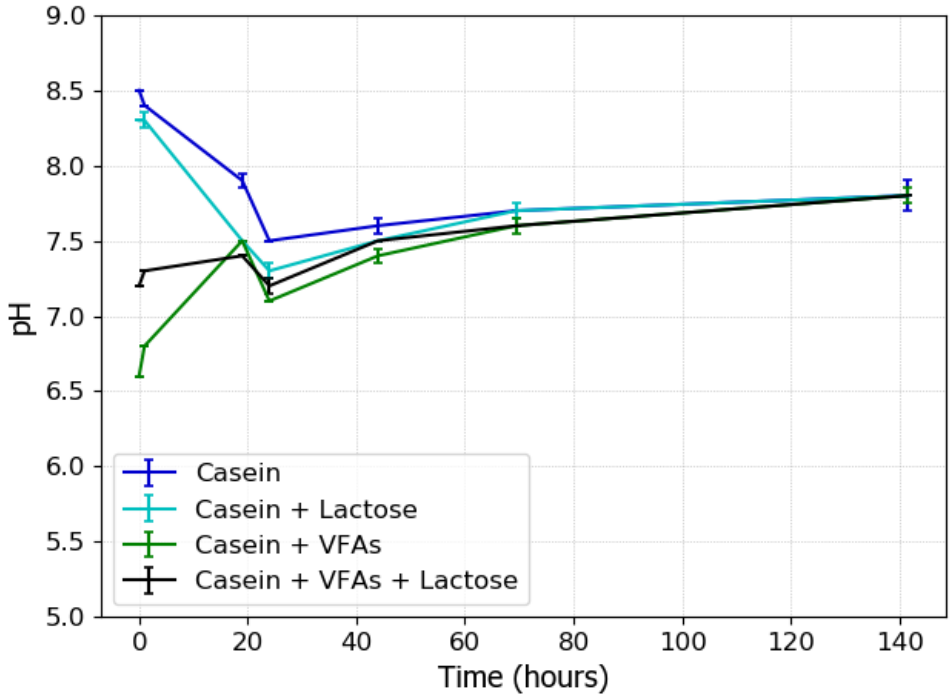

Figure B.4: pH data over a period of 140 hours for casein (dark blue), casein + lactose (cyan), casein + VFAs (green) and casein + VFAs + lactose (black).

B.4 VOLATILE FATTY ACIDS PROFILES OF ACIDIFICATION TRIALS

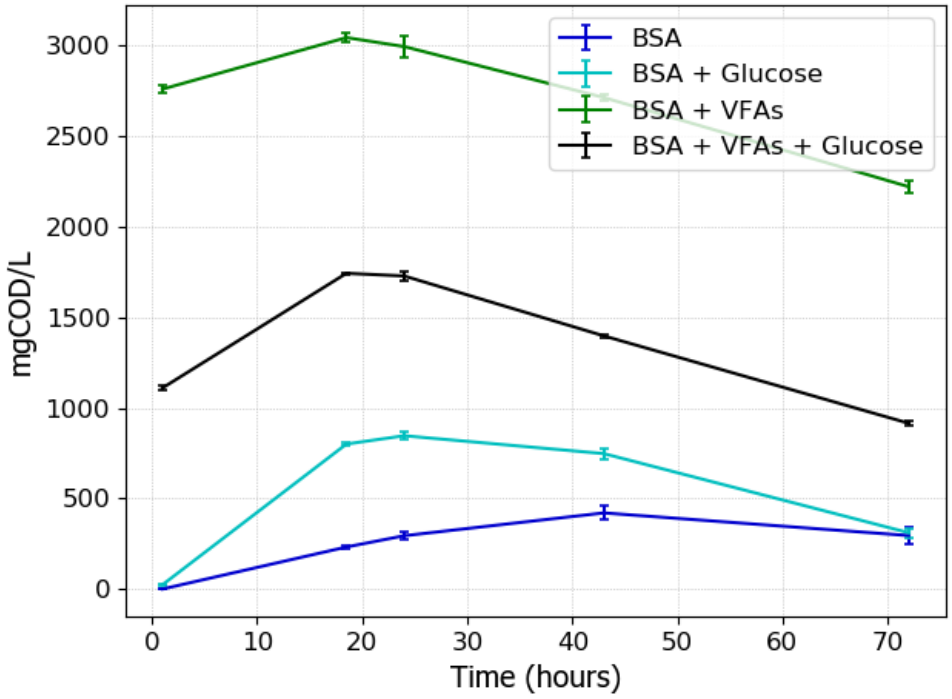

Figure B.5: VFA data over a period of 72 hours for the acidification trial of BSA. The represented substrates are BSA (dark blue), BSA + glucose (cyan), BSA + VFAs (green) and BSA + VFAs + glucose (black).

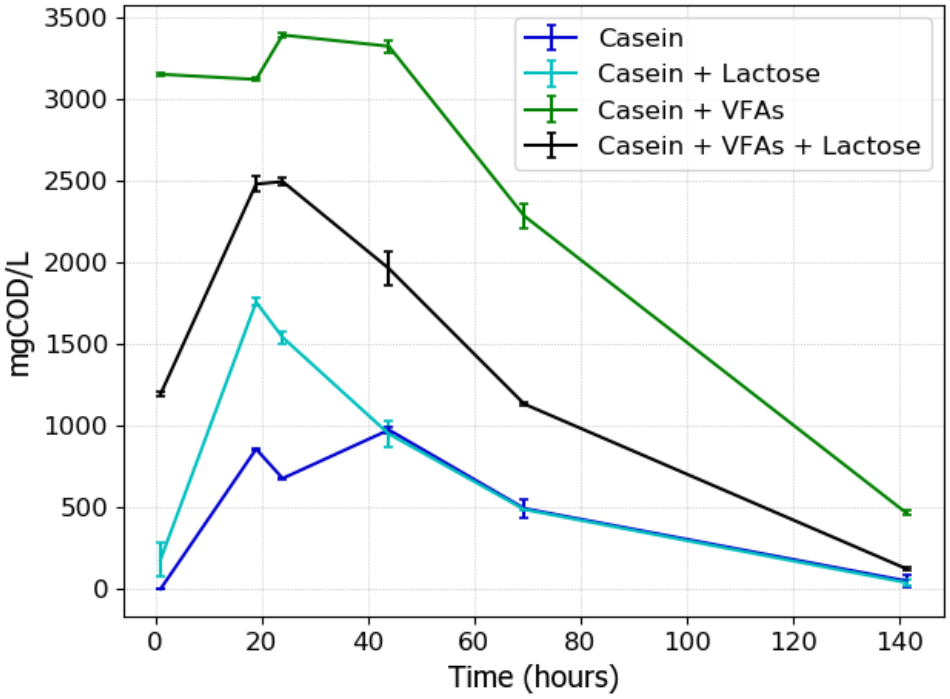

Figure B.6: VFA data over a period of 140 hours for the acidification trial of casein. The represented substrates are casein (dark blue), casein + lactose (cyan), casein + VFAs (green) and casein + VFAs + lactose (black).

B.5 COD AND NITROGEN MASS BALANCES

B.5.1 Batch 2: Gelatin and BSA

B.5.2 Batch 3: Gelatin and casein

In table B.9 it can be seen that the casein trial did not yield any biogas. This is due to a technical issue where one of the bottles with casein showed a gas leakage and therefore no representative amount of biogas was produced.

Table B.6: Nitrogen balance for the first gelatin and BSA trials

	SKN_{ini} (mgN/L)	SKN_{fin} (mgN/L)	dosed NH4 (mgNH4-N/L)	$Protein_{ini}$ (mgN/L)	$Protein_{fin}$ (mgN/L)	$NH4_{ini}$ (mgNH4-N/L)	$NH4_{fin}$ (mgNH4-N/L)	Fraction N in protein (%)	Nitrogen balance (%)
Gelatin	1166.25	783.63	29.60	1028.51	63.93	5.95	865.93	17.82	92.49
BSA	921.68	895.65	231.31	1052.48	185.14	6.69	877.93	17.79	115.34
BSA + Glucose	983.90	816.97	588.15	581.04	22.06	110.35	876.93	17.79	91.37

Table B.7: COD balance for the first gelatin and BSA trials. COD going into biomass was taken as 5% from the initial COD concentration. Values of biogas COD were calculated with biogas volumes after t = 137h when the last liquid sample was also taken.

	COD_{ini} (mgCOD/L)	COD_{biogas} (mgCOD/L)	COD_{eff} (mgCOD/L)	$COD_{biomass}$ (mgCOD/L)	Methanised COD (%)	COD balance (%)
Gelatin	6195.79	5606.29	581.15	309.79	100.21 $\pm$ 0.55	104.87
BSA	6345.29	5025.14	769.90	317.26	79.19 $\pm$ 0.5	96.33
BSA + Glucose	5954.29	5001.43	366.40	297.71	84.00 $\pm$ 2.22	95.15

B.5.3 Batch 4: Acidification of BSA

B.5.4 Batch 5: Acidification of casein

Table B.8: Nitrogen balance for the first gelatin and casein trials

	SKN_{ini} (mgN/L)	SKN_{fin} (mgN/L)	dosed NH4 (mgNH4-N/L)	$Protein_{ini}$ (mgN/L)	$Protein_{fin}$ (mgN/L)	$NH4_{ini}$ (mgNH4-N/L)	$NH4_{fin}$ (mgNH4-N/L)	Fraction N in protein (%)	Nitrogen balance (%)
Gelatin	857.40	858.11	25.60	853.58	108.88	2.64	842.75	17.82	111.33
Gelatin + Glucose	890.73	947.99	415.70	443.72	41.16	60.45	870.50	17.82	104.41
Casein	822.35	775.00	1.77	899.71	296.41	7.66	800.25	15.91	130.14
Casein + Lactose	873.27	725.69	413.94	546.23	144.78	18.85	788.50	15.91	113.06

Table B.9: COD balance for the first gelatin and casein trials. COD going into biomass was taken as 5% from the initial COD concentration. Values of biogas COD were calculated with biogas volumes after t = 230h.

	COD_{ini} (mgCOD/L)	COD_{biogas} (mgCOD/L)	COD_{eff} (mgCOD/L)	$COD_{biomass}$ (mgCOD/L)	Methanised COD (%)	COD balance (%)
Gelatin	6006.45	5487.71	975.40	300.32	95.16 $\pm$ 0.94	112.60
Gelatin + Glucose	6277.70	5504.29	498.15	313.89	92.10 $\pm$ 0.21	100.62
Casein	7759.20	0.00	2261.40	387.96	0.00	34.14
Casein + Lactose	6718.70	5503.43	838.15	335.94	81.91 $\pm$ 0.67	99.39

Table B.10: Nitrogen balance for the BSA acidification trial.

	SKN_{ini} (mgN/L)	SKN_{fin} (mgN/L)	dosed NH4 (mgNH4-N/L)	$Protein_{ini}$ (mgN/L)	$Protein_{fin}$ (mgN/L)	$NH4_{ini}$ (mgNH4-N/L)	$NH4_{fin}$ (mgNH4-N/L)	Fraction N in protein (%)	Nitrogen balance (%)
BSA	321.18	302.84	8.89	444.65	78.38	0.19	292.53	17.79	115.92
BSA + Glucose	297.66	259.13	19.77	513.83	90.23	6.88	257.28	17.79	117.94
BSA + VFAs	699.15	648.17	388.48	485.17	85.29	1.72	649.78	17.79	111.56
BSA + Glucose + VFAs	709.92	663.17	409.23	482.21	96.17	3.96	679.53	17.79	121.87

Table B.11: COD balance for the BSA acidification trial. COD going into biomass was taken as 5% from the initial COD concentration. Values of biogas COD were calculated with biogas volumes after t = 230h.

	COD_{ini} (mgCOD/L)	COD_{biogas} (mgCOD/L)	COD_{eff} (mgCOD/L)	$COD_{biomass}$ (mgCOD/L)	Methanised COD (%)	COD balance (%)
BSA	3016.00	2426.29	907.45	145.00	91.08 $\pm$ 0.68	115.34
BSA + Glucose	6315.70	5070.29	930.95	315.79	87.38 $\pm$ 0.13	100.02
BSA + VFAs	6224.95	3107.43	458.80	311.25	86.84 $\pm$ 2.18	62.29
BSA + Glucose + VFAs	6147.45	4564.86	761.40	307.37	87.38$\pm$ 0.30	91.64

Table B.12: Nitrogen balance for the casein acidification trial.

	SKN_{ini} (mgN/L)	SKN_{fin} (mgN/L)	dosed NH4 (mgNH4-N/L)	$Protein_{ini}$ (mgN/L)	$Protein_{fin}$ (mgN/L)	$NH4_{ini}$ (mgNH4-N/L)	$NH4_{fin}$ (mgNH4-N/L)	Fraction N in protein (%)	Nitrogen balance (%)
Casein	284.85	-	5.93	491.62	119.72	0.84	299.50	15.91	148.18
Casein + Lactose	253.07	-	0.49	487.64	137.62	1.20	275.50	15.91	163.37
Casein + VFAs	696.20	-	345.97	491.82	159.50	11.61	613.25	15.91	121.86
Casein + Lactose + VFAs	717.75	-	387.49	579.32	147.57	-3.70	651.75	15.91	124.70

Table B.13: COD balance for the casein acidification trial. COD going into biomass was taken as 5% from the initial COD concentration. Values of biogas COD were calculated with biogas volumes after t = 230h.

	COD_{ini} (mgCOD/L)	COD_{biogas} (mgCOD/L)	COD_{eff} (mgCOD/L)	$COD_{biomass}$ (mgCOD/L)	Methanised COD (%)	COD balance (%)
Casein	3185.10	2436.57	507.20	159.26	84.25 $\pm$ 15.5	97.42
Casein + Lactose	6121.85	5631.14	686.70	306.09	90.81 $\pm$ 3.52	108.20
Casein + VFAs	5239.60	4951.43	706.20	261.98	92.58 $\pm$ 1.58	112.98
Casein + Lactose + VFAs	5540.85	4911.43	744.70	277.04	84.42 $\pm$ 0.87	107.08

B.6 BMP OF ACIDIFICATION TRIALS

Table B.14: The average total yield of methane (NL) produced per kilogram of COD and biodegradability of the acidification trial of BSA. The BMP yield was calculated with equation 4.10, whereas the formula used for biodegradability is 4.11.

	Averaged BMP yield (NL_{CH4}/kg_{COD})	Theoretical methane yield (NL_{CH4}/kg_{COD})	Biodegradability
BSA (25% acidification) (n = 2)	290 ± 1	350	87.4 ± 0.3%
BSA (50% acidification) (n = 2)	290 ± 8	350	86.8 ± 2.2%

Table B.15: The average total yield of methane (NL) produced per kilogram of COD and biodegradability of the acidification trial of casein. The BMP yield was calculated with equation 4.10, whereas the formula used for biodegradability is 4.11.

	Averaged BMP yield (NL_{CH4}/kg_{COD})	Theoretical methane yield (NL_{CH4}/kg_{COD})	Biodegradability
Casein (25% acidification) (n = 2)	298 ± 4	350	84.4 ± 0.9%
Casein (50% acidification) (n = 2)	317 ± 6	350	92.6 ± 1.6%

COLOPHON

This document was typeset using LaTeX. The document layout was generated using the arsclassica package by Lorenzo Pantieri, which is an adaption of the original classicthesis package from André Miede.